PLOS ONE

DNA methylation characteristics of primary melanomas with distinct biological behaviour

--Manuscript Draft--

Manuscript Number:	PONE-D-13-50067R1
Article Type:	Research article
Full Title:	DNA methylation characteristics of primary melanomas with distinct biological behaviour
Short Title:	DNA methylation in primary melanomas
Corresponding Author:	Margit Balazs, Ph.D. D.Sc. Medical and Health Science Center, University of Debrecen Debrecen, Hajdú-Bihar HUNGARY
Keywords:	primary melanoma, tumour progression, epigenetics, DNA methylation, hypermethylation, hypomethylation, copy number alteration, array CGH, BRAF mutation
Abstract:	In melanoma, the presence of promoter related hypermethylation has previously been reported, however, no methylation-based distinction has been drawn among the diverse melanoma subtypes. Here, we investigated DNA methylation changes associated with melanoma progression and links between methylation patterns and other types of somatic alterations, including the most frequent mutations and DNA copy number changes. Our results revealed that the methylome, presenting in early stage samples and associated with the BRAFV600E mutation, gradually decreased in the medium and late stages of the disease. An inverse relationship among the other predefined groups and promoter methylation was also revealed except for histologic subtype, whereas the more aggressive, nodular subtype melanomas exhibited hypermethylation as well. The Breslow thickness, which is a continuous variable, allowed for the most precise insight into how promoter methylation decreases from stage to stage. Integrating our methylation results with a high-throughput copy number alteration dataset, local correlations were detected in the MYB and EYA4 genes. With regard to the effects of DNA hypermethylation on melanoma patients' survival, correcting for clinical cofounders, only the KIT gene was associated with a lower overall survival rate. In this study, we demonstrate the strong influence of promoter localized DNA methylation changes on melanoma initiation and show how hypermethylation decreases in melanomas associated with less favourable clinical outcomes. Furthermore, we establish the methylation pattern as part of an integrated apparatus of somatic DNA alterations.
Order of Authors:	Szilvia Irina Ecsedi
	Hector Hernandez-Vargas
	Sheila Coelho Lima
	Laura Vizkeleti
	Reka Toth
	Viktoria Lazar
	Viktoria Koroknai
	Timea Kiss
	Gabriella Emri
	Zdenko Herceg
	Roza Adany
	Margit Balazs, Ph.D. D.Sc.
Suggested Reviewers:	Michael Murphy, PhD

	Associate Professor, University of Connecticut mimurphy@nso1.uchc.edu
	Jan Betka Charles University, Prague Jan.Betka@lfmotol.cuni.cz
Opposed Reviewers:	
Response to Reviewers:	RESPONSE FOR REVIEWS First we would like to thank both Reviewers for thoroughly reviewing our manuscript. According to the suggestions of Reviewer 1, we checked our manuscript for spelling mistakes and furthermore, for the Academic Editor's requests and according to the suggestions of Reviewer 2, we reorganized some critical points in our manuscript and performed the additional signalling analysis has been requested. The title of our manuscript has been changed as well. The new title is "DNA methylation characteristics of primary melanomas with distinct biological behaviour". It was also essential to rewrite some parts of the "Materials and Methods", "Results" and the "Discussion" sections parts. We believe that the improved version of our manuscript will meet the high standards of the PLOS One Journal. We have answered all the comments and the questions one by one. For improved understanding we have listed the original notes and questions in bold italic and the answers in normal fonts. Among our answers, all additional descriptions we would like to add into the revised version have been marked by underlined titles and italic fonts. REVIEWER 2 Major comments 1. The title of the manuscript is "DNA methylation is more characteristic of melanoma initiation than progression". However, the whole study did not show DNA methylation, melanoma initiation, and progression at all except for figure 2. The whole study needs to be focused on one theme. According to the Reviewer's suggestion, the title of our manuscript was changed for "DNA methylation characteristics of primary melanomas with distinct biological behaviour". We hope that the new title may reflect better the comprehensive analysis of our studies aiming at providing a general view in how DNA methylation associates with the distinct clinical characteristics of primary melanoma and how it accompanied by other somatic alterations. Although we attempted to evaluate whether DNA methylation contributes to other somatic alterations such as well-known mutations and copy number changes, considering possible crosstalk between the aforementioned alterations, we believe that our goals are still focused on one theme in a genomic and epigenomic scale and our results may provide improved insights into more generalized mechanisms at work in carcinogenesis. 2. Authors performed data analysis using false discovery rate cut off of 20%. Is it stringent enough? As of yet no conventions have been established for false discovery rate (FDR) in published work, an FDR of 5 or 10% is generally chosen by studies performed at genome scale, however, considering a preselected nature of Illumina GoldenGate Cancer Panel I which is enriched in cancer related genes, a less stringent FDR value can be also acceptable [1]. 3. In figure 1, authors showed the DNA methylation patterns according to different clinical predictors. What kind of data do the authors show in figure 1A? For an example, for Breslow thickness group, according to table 1, there are three size categories. Which dots are representing each class? Also where are the red dots? What does the X axis mean? Page 9, paragraph 2, authors interpreted that "Figure 1A

demonstrates that relatively large number of CpG was found to be differential methylated … in both superficial and nodular subtype." However, from the figure 1A, most of the CpG do not show significant differences at all. This figure is so confused. I can not figure out how the authors see a disturbed methylation pattern in superficial and nodular subtype (page 9).

We are very sorry if Figure 1 was not clear in the original manuscript. Figure 1A-D represent volcano plots for the methylation level of CpG sites in relation with Breslow thickness, Metastatic capacity, Ulceration and Histologic subtype. This type of plot was originally developed to illustrate gene expression data, however, several publications have chosen Volcano plots to depict differential DNA methylation data as well [2,3]. The volcano plot arranges genes along dimensions of biological and statistical significance. The first (horizontal) dimension is the relative difference between the methylation of two given groups on a log scale; consequently, hypo and hypermethylation appear symmetric. In this case, it is crucial to emphasize that samples with worse prognoses were compared to samples with better prognosis. (If samples that are characteristic for favourable prognosis are compared to samples with worse prognosis, the differentially methylated genelist will remain the same, but turn backward in position.) The second (vertical) axis represents the p-value for a t-test of differences between samples (most conveniently on a negative log scale – so smaller p-values appear higher up). For improved understanding and to avoid misleading of readers, we reedited Figure 1 in a coloured style (see below, p.3) and clearly indicated the p-value cut-off (based on t-tests corrected for FDR) by a horizontal green line, whereas vertical green line was inserted to separate direction to decreased - and increased DNA methylation (therefore, dots are not specific for samples but mark individually the differentially methylated genes). To visualize the overlap between the differentially methylated genes in each clinical subgroup, we created individual Venn diagrams specific for hypo- and hypermethylation, respectively. Notably, the new Supplementary Table 1 corroborates Figure 1 providing detailed gene lists with fold change values; the rate of fold change clearly shows if a methylation level of a given gene decrease or increase in relation with tumour progression categories.
The following text was inserted into the Results section in order to provide better description of Figure 1 (p.9, line 10):
"Figure 1A demonstrates that relatively large number of CpG sites was found to be differentially methylated between melanoma subgroups. Interestingly, the majority of these CpGs were characterised by decreased DNA methylation levels in samples with poor prognosis (larger than 4 mm, metastatic, ulcerated and nodular primary melanomas). Histologic subtype exhibited a more disturbed methylation pattern involving high number of differentially methylated genes in both superficial and nodular subtype. As it can be seen in Figure 1A, some of the differentially methylated individual genes were represented by more than one significant CpG sites arguing in favour of the consistency of given alterations. Altogether, 111 differentially methylated genes were identified in the context of aforementioned clinical predictors: 43 individual genes were hypermethylated and 68 genes hypomethylated in melanomas with less favourable clinical outcome. The differentially methylated gene lists specific for the Breslow thickness, ulceration, metastatic capacity and histologic subtype are detailed in Supplementary Table 1. Venn diagrams (Figure 1B) indicate the common properties among genes with decreased and increased DNA methylation, respectively."

Figure 1 DNA Methylation patterns of primary melanomas with known clinical predictors
(A) Volcano plots of differentially methylated genes associated with known predictors. Blue dots indicates decreased and red indicates increased methylation as follows: Breslow thickness: 51 hypomethylated probes (43 individual genes) and 5 hypermethylated probes (5 individual genes); metastatic capacity: 23 hypomethylated probes (21 individual genes) and 5 hypermethylated probes (4 individual genes), ulceration: 48 hypomethylated probes (43 individual genes) and 8 hypomethylated probes (8 individual genes), histologic subtype: 28 hypomethylated probes (26 individual genes) 23 hypermethylated probes (20 individual genes) (B) A Venn diagrams indicate the overlap of differentially methylated genes (in left: number of

hypomethylated genes; in right: number of hypermethylated genes) for each clinical predictor class.

Figure 1 DNA Methylation patterns of primary melanomas with known clinical predictors
(A) Volcano plots of differentially methylated genes associated with known predictors. Blue dots indicates decreased and red indicates increased methylation as follows: Breslow thickness: 51 hypomethylated probes (43 individual genes) and 5 hypermethylated probes (5 individual genes); metastatic capacity: 23 hypomethylated probes (21 individual genes) and 5 hypermethylated probes (4 individual genes), ulceration: 48 hypomethylated probes (43 individual genes) and 8 hypomethylated probes (8 individual genes), histologic subtype: 28 hypomethylated probes (26 individual genes) 23 hypermethylated probes (20 individual genes) (B) A Venn diagrams indicate the overlap of differentially methylated genes (in left: number of hypomethylated genes; in right: number of hypermethylated genes) for each clinical predictor class.

Although the clinicopathological characteristics of primary melanomas were summarized in Table 1, regarding Breslow thickness (which is a continuous variable measured in millimetres) we further clarified it in Table 1 (see at p5) and indicated that melanoma thickness can be categorized into two or either more groups according to the clinical practise [4,5]. On binary data (each class are binary shown in Figure 1), t-test was used as indicated in the Materials and Methods section.

For better following of statistical analysis and illustrations, the following part was inserted into the “Materials and Methods” section (p.7, line 13):

Statistical analysis
“To compare the methylation patterns between primary melanoma groups detailed in Table 1, we applied random variance t-statistics on all the binary data classes such as Breslow thickness with the cut-off value of 4 mm; metastasis, ulceration and histologic subtype. Being continuous variable, Breslow thickness can be divided into more subgroups: according to the TNM system up to 5 groups can be created, however, due to the limitation of smaller samples, developing 3 groups based on the cut-off values of 2mm and 4mm were the most ideal. F-statistics was applied on the trichotomised Breslow groups for each CpG site.
CpG sites were considered differentially methylated when their p values based on univariate t-tests or f-tests were less than 0.01; in addition, given CpG sites were identified differentially methylated between the melanoma subgroups based on a multivariate permutation test providing 90% confidence that the false discovery rate was less than 20%. Volcano plots were applied to illustrate differential methylation patterns among clinical subgroups of melanomas (the clinicopathological characteristics of melanomas are summarized in Table 1). Volcano plots combine p-values of the t-tests for each CpG sites and ratios between the melanoma subgroups. Additionally, the trichotomised Breslow thickness groups were visualized by heatmap and compared by Principal Component Analysis (PCA).
For the aforementioned class comparisons, M-values, the logit transformations of signal intensities were used.”

Table 1. Clinical-pathological parameters of primary melanomas

Variables	No. of tumours analysed by Illumina bead assay
All patients	42
Histological subtype	
SSM1	26
NM2	16
Gender	
Female	20
Male	22
Age (years)	
20-50	14
≥50	28
Breslow thickness (mm)3	
≤4	26
>4	16
Breslow thickness (mm)4	
≤2	15
2-4	11
>4	16
Location of primary tumour	
Extremity	21
Trunk	20
Head	1
Metastasis formation5	
Absent	20
Present	22
Patient’s survival6	
Alive	21
Exitus	21
Ulceration	
Absent	20
Present	22
BRAFV600E mutation	
BRAFV600E mutant	12
BRAFV600E wild type	24

1Superficial spreading melanoma.2Nodular melanoma.3Thickness categories are based on the current staging system. 4Thickness categories are based on the current staging system.5Metastasis of the examined primary tumours. 6Patients with at least a 5-year follow-up period were included.

4. Figure 2, authors showed the differences in DNA methylation during different stages. How about DNA methylation changes for other subtypes? Also, how did authors pick the 45 CpGs? Why does the middle panel for figure 2A have fewer CpGs for the same gene?

As written above (see Answers for Question 2), the DNA methylation changes for all the subtypes of melanomas (Breslow thickness, Histological subtype, Metastatic capacity and Ulceration) were computed based on t-tests for each CpG values and adjusted for FDR and finally shown by Volcano plots which combine the p-values and fold changes between the given subgroups. Among clinical properties of melanomas, Breslow thickness is measured in millimetres. Being a continuous variable, Breslow thickness provides a unique opportunity to create more than two groups. In the clinical practice, Breslow thickness can be dichotomised by the cut-off value of 4 mm (melanomas larger than 4mm reflects the worst prognosis) or more commonly, divided into three groups by the cut-off values of 2 mm and 4 mm [4,5].

Altogether, the data in which the statistical comparison were made are the same compared to those which are indicated in Figure 1A, however, on trichotomised data, f-tests should be used instead of t-test, which results in a slightly different number of methylated genes among thin, medium and thick melanomas compared to results depicted in Figure 1A. Nonetheless, the overlap between the two approaches (statistics on dichotomised vs. trichotomised datasets) is above 80% and the latter approach provides a unique opportunity to illustrate the dynamics of DNA methylation changes over melanoma progression.

5. Authors looked at pathways without explaining how they performed the analysis. Authors should use the genes shown differences in DNA methylation in figure 2 to look for the pathways that might be perturbed during melanoma progression.

It is interest of seeing that melanoma bearing BRAF mutation has different methylated gene patterns. What is the relationship between BRAF mutation and melanoma initiation and progression? Authors should present the rationale for each analysis in the main text.

We used Efron-Tibshirani GSEA (Gene Set Enrichment Analysis) maxmean statistical approach which is implemented into BRB Array Tools Software. The entire background of GSEA maxmean test was published by Tibshirani et al [6]. Briefly, the t-statistics of zj for all genes in our data are computed, where zk = (z1, z2, . . . , zm) is the gene scores for the m genes in a geneset Sk. Then a gene-set score Sk(zk) for each gene-set Sk is computed equal to essentially a signed version of the Kolmogorov–Smirnov statistic between the values {zj, j ∈ Sk} and their complement {zj, j /∈ Sk}; the sign taken positive or negative depending on the direction of shift. The idea is that if some or all of the gene-set Sk have higher (or lower) values of zj than expected, their summary score Sk should be large. An absolute cut-off value is defined, and values of Sk above (or below) the cutoff are declared significant. The GSEA method then performs many permutations of the sample labels and recomputes the statistic on each permuted dataset.

According to the Reviewer's suggestion, besides the comparison of BRAFV600E and wild type melanomas, we extended our signalling analysis to each clinical subgroups and found lack of enrichment involving exclusively a single signalling pathway being enriched for ulcerated and one melanomas. Therefore, we reedited Figure 3 with legends as follows:

Figure 3 Differentially methylated gene sets between melanoma classes
(A) Differentially methylated gene sets between BRAFV600E mutant and wild-type, metastatic and non-metastatic, ulcerated and non-ulcerated classes according to the Kyoto Encyclopaedia of Genes and Genomes. (B) Average log-ratios of methylation intensities in BRAFV600E mutant and wild-type melanomas. Red indicates significant genes associated with ECM-receptor interaction and blue depicts significant genes on Cell communication pathway. (Eleven genes overlap between the ECM-receptor

interaction and Cell communication.) (C) Venn diagram shows lack of overlap between differentially methylated genes associated with BRAFV600E mutation and the known clinical predictors as Breslow thickness, metastatic capacity, ulceration and histologic subtype.

Corrected parts of the Results section:
“In addition to individual gene signatures, we aimed to determine whether the perturbed KEGG-based gene networks are related to localised methylation patterns. We identified differentially methylated genes belongs to Cell cycle pathways in primary melanomas with metastatic capacity. Genes associated at Leukocyte signalling were also demonstrated to be differentially methylated in ulcerated samples (Figure 3A). Interestingly, Cell communication and ECM-receptor interaction networks were found to be significant at the 0.01 level between BRAFV600E mutant and wild type samples, notwithstanding the fact that, we was unable to find differentially methylated CpGs at the individual gene level (Figure 3A-B). The full list of CpG probes is given in Supplementary Table 2. There was poor overlap (Figure 3C) between the differentially methylated genes associated with BRAFV600E mutation and clinical subgroups discussed above”.

Apart from the single study on melanoma cell lines – mentioned in our “Discussion” section – the association between DNA methylation and activating BRAF mutations in colon cancer has been identified [7]. Based on these investigations the following part has been inserted into the “Discussion” section (p.15, line 24):

“A remarkable study performed by Roon et al. revealed the BRAFV600E mutation-specific hypermethylation of CpG regions in colon cancer samples by Differential Methylation Hybridization on high-density oligonucleotide microarrays. Interestingly, the authors identified several cancer-related pathways, including the PI3 kinase and Wnt signaling pathways being differentially methylated between BRAFV600E mutant and wild type samples. Additionally, the group found the silencing of FOXD3 hypermethylated manner. Based on these studies, authors suggest that a specific epigenetic pattern can contribute to a favorable context for the acquisition of BRAFV600E mutations. However, further studies are warranted to further clarify the relationship between the mutation and DNA methylation.”

6. Authors performed qPCR for measuring mRNA expression of a couple of genes. Authors should perform RNA-seq or microarray to measure gene expression alteration during different stages of progression.

We have to agree with the Reviewer that mRNA-seq is the most accurate method for gene expression measurement. However, we used qPCR to measure the gene expression of exclusively some of those genes that were altered by methylation. For decades, qPCR has been the gold standard for detecting mRNA expression of specific genes. Recently, RNA-seq, the robust and highly reliable method has been introduced and in the field of melanoma research the technique is still pioneering and only a few results have been published so far summarized by Dannemann et al [8]. Nonetheless, the published data on samples other than melanoma showed that RNA-seq and qPCR results highly correlated suggesting the reproducibility of qPCR experiments [9]. Apart from the numerous advantages and improved insights provided by the RNA-seq method, our goal was to validate our DNA methylation results on a gene expression level in randomly selected genes rather than provide a systematic, genome scale comparison between methylation and mRNA expression.

7. Figure legend of figure 6 needs to be clarified. Authors wrote “Red indicated CN losses and green indicated CN gains”. However, where is the green? What does shaded area mean? It seems that DNA methylation is everywhere and at a similar level? Authors need to quantify the DNA methylation and CN changes. Also authors should compare that among samples from different stages in order to correlation DNA mehtyaltion, CN changes, and melanoma progression?

The copy number aberrations over all of our primary melanoma dataset were quantified according to the GISTIC (Genomic Identification of Significant Targets in Cancer), designed for analysing chromosomal aberrations specifically in cancer based

on the following method:
The so-called G scores involve both the frequency of occurrence and the amplitude of the copy number aberration [10]. The algorithm also assesses the statistical significance of each aberration by comparing the observed statistic to the results that would be expected by chance, using a permutation test that is based on the overall pattern of aberrations seen across the genome. The statistical approach method adjusts for multiple-hypothesis testing using the false-discovery rate (FDR) and assigns a q value to each result, reflecting the probability that the event is due to chance fluctuation [10]. Using GISTIC, the common chromosome arm-level events are omitted and the more informative so-called “focal events” or in other word, the “peak regions” of significance are determined (depicted by grey lines at Figure 6) with their boundaries, the so-called “extended regions” which are indicated by the grey shaded area. Calculating of the aforementioned boundaries is based on leaving each sample out in turn, and recalculating the peak boundaries.

Based on the suggestions of Reviewer 2, we corrected the legend of Figure 6 as follows:

Figure 6 Coincidence of DNA copy number (CN) alterations and disturbed methylation pattern in BRAFV600E mutant melanomas
(A) The distribution of CN aberrations (red indicates CN losses and blue indicates CN gains on the frequency plot) specific for the BRAFV600E mutant (purple line on the left) and BRAFV600E wild-type (green line on the left) primary melanomas. The methylated genes are shown as blue lines in the lower part of the figure, and the red dotted circle highlights 6q23 as the only region where a coincidence was revealed. The significant CN alterations are highlighted in grey in the upper part of the figure. Frequent CN losses (B) and CN gains (C) are given based on the G-score of GISTIC algorithm, which is a measure of the frequency of occurrence of the aberration and the magnitude of the CN alteration at each location in the aggregate of all samples in the dataset. The locations of the alterations in each sample are permuted, simulating data with random aberrations, and the significance is represented as Q-Bounds. Grey lines indicate the peak, whereas the grey shaded area is an extended peak based on leave-one-out algorithm to allow for errors in the boundaries in a single sample. (C) Correlation plot for CN alterations and DNA methylation regarding the MYB gene and (D) the EYA4 gene.

With comparing copy number changes to DNA methylation results, our aim was to highlight associations between the distinct types of somatic alterations. Association was exclusively found to be related to BRAF V600E mutation. Additional copy number changes (without coordinate differentially methylation) are reported also in Figure 6 (between BRAFV600E mutant and wild type samples) and in Supplementary Figure 1 (between small, medium and large primary melanomas according to the trichotomised Breslow thickness categories).

Minor comments
1. What are the M-values and Avg-Beta values? Authors should explain what they are when they first introduce in the text. The same thing for OS values for figure 4.

Based on the Reviewer’s suggestion, the “Bead Assay Experiment” part of the “Materials and Methods” section has been completed as well (p.5, line 24) as the legend of Figure 4 to clearly explain the meaning of AVG-Beta values, M-values and OS.

Bead Assay experiments
“The quantitative methylation status of the 1505 CpG sites corresponding to 807 cancer-related gene promoters was determined using the Illumina GoldenGate Methylation Assay (Illumina, San Diego, CA, USA) on bisulphite-treated DNA samples corresponding to 42 primary melanomas. Bisulphite treatment was performed on 500 ng DNA using the EZ DNA Methylation-Gold Kit (Zymo Research). Duplicate samples were included to measure inter-array reproducibility for quality control. The GoldenGate assay consists of two allele-specific oligos (ASO) and two locus-specific oligos (LSO) for each CpG site. Each ASO–LSO oligo pair corresponds to either the methylated or unmethylated state of the CpG site. Each methylation CpG spot is represented by two-

	color fluorescent signals from the M (methylated) and U (unmethylated) alleles. BeadStudio version 3.2 (Illumina) was used for obtaining the signal values (Avg-Beta) corresponding to the ratio of the fluorescent signal from the methylated allele (Cy5) to the sum of the fluorescents signals of both methylated (Cy5) and unmethylated alleles (Cy3), 0 corresponding to completely unmethylated sites and 1 to completely methylated sites. In agreement with the literature, 83 probes corresponding to the sex chromosomes were excluded to avoid any sex-specific bias. The probes with detection P values exceeding 0.01 in more than 10% of the specimens were removed from the analyses to exclude non-biological differences. As Du et al. performed a systematic comparison between Avg-Beta values and M-values, which is the logit transformation of Avg-Beta, and M-values were proven to be statistically valid for conducting differential methylation analysis[11], M-values were used for class comparisons, whereas the raw Avg-Beta values were applied for correlation analyses (see at “Statistical Analysis”).” Figure 4 Hypermethylated genes associated with decreased survival rate in melanoma patients The Kaplan-Meier curves for genes (DSP, EPHB6, HCK, IL18, IRAK3 and KIT) whose hypermethylation was associated with a lower overall survival rate (OS); the Cox proportional univariate approach was performed on each gene to test whether a methylation status of a particular gene significantly influences the survival at the $p < 0.05$ level. References 1. Hernandez-Vargas H, Ouzounova M, Le Calvez-Kelm F, Lambert MP, McKay-Chopin S, et al. (2011) Methylome analysis reveals Jak-STAT pathway deregulation in putative breast cancer stem cells. Epigenetics 6: 428-439. 2. Christensen BC, Houseman EA, Poage GM, Godleski JJ, Bueno R, et al. (2010) Integrated profiling reveals a global correlation between epigenetic and genetic alterations in mesothelioma. Cancer Res 70: 5686-5694. 3. Nischal S, Bhattacharyya S, Christopeit M, Yu Y, Zhou L, et al. (2013) Methylome profiling reveals distinct alterations in phenotypic and mutational subgroups of myeloproliferative neoplasms. Cancer Res 73: 1076-1085. 4. Fisher NM, Schaffer JV, Berwick M, Bolognia JL (2005) Breslow depth of cutaneous melanoma: impact of factors related to surveillance of the skin, including prior skin biopsies and family history of melanoma. J Am Acad Dermatol 53: 393-406. 5. Guitera P, Li LX, Crotty K, Fitzgerald P, Mellenbergh R, et al. (2008) Melanoma histological Breslow thickness predicted by 75-MHz ultrasonography. Br J Dermatol 159: 364-369. 6. Efron B TR (2007) On testing the significance of sets of genes. Ann Appl Stat: 107-129. 7. van Roon EH, Boot A, Dihal AA, Ernst RF, van Wezel T, et al. (2013) BRAF mutation-specific promoter methylation of FOX genes in colorectal cancer. Clin Epigenetics 5: 2. 8. Kunz M, Dannemann M, Kelso J (2013) High-throughput sequencing of the melanoma genome. Exp Dermatol 22: 10-17. 9. Wang Z, Gerstein M, Snyder M (2009) RNA-Seq: a revolutionary tool for transcriptomics. Nat Rev Genet 10: 57-63. 10. Beroukhim R, Getz G, Nghiemphu L, Barretina J, Hsueh T, et al. (2007) Assessing the significance of chromosomal aberrations in cancer: methodology and application to glioma. Proc Natl Acad Sci U S A 104: 20007-20012. 11. Du P, Zhang X, Huang CC, Jafari N, Kibbe WA, et al. (2010) Comparison of Beta-value and M-value methods for quantifying methylation levels by microarray analysis. BMC Bioinformatics 11: 587.
Additional Information:	
Question	**Response**
Competing Interest For yourself and on behalf of all the	The authors have declared that no competing interests exist

authors of this manuscript, please declare below any competing interests as described in the "PLoS Policy on Declaration and Evaluation of Competing Interests." You are responsible for recognizing and disclosing on behalf of all authors any competing interest that could be perceived to bias their work, acknowledging all financial support and any other relevant financial or competing interests. If no competing interests exist, enter: "The authors have declared that no competing interests exist." If you have competing interests to declare, please fill out the text box completing the following statement: "I have read the journal's policy and have the following conflicts" * typeset	
Financial Disclosure Describe the sources of funding that have supported the work. Please include relevant grant numbers and the URL of any funder's website. Please also include this sentence: "The funders had no role in study design, data collection and analysis, decision to publish, or preparation of the manuscript." If this statement is not correct, you must describe the role of any sponsors or funders and amend the aforementioned sentence as needed. * typeset	Grant sponsor: This research was supported by the Hungarian National Research Fund (OTKA K75191), the Hungarian Academy of Sciences (grant number 2011 TKI 473), the UD Faculty of Medicine Research Fund (Bridging Fund 2012), the TÁMOP-4.2.2/B-10/1-2010-0024 and TÁMOP-4.2.2.A-11/1/KONV-2012-0031 projects; the TÁMOP projects are co-financed by the European Union and the European Social Fund. The authors have no connection with any of the companies or products mentioned in this article. The funders had no role in study design, data collection and analysis, decision to publish, or preparation of the manuscript.
Ethics Statement All research involving human participants must have been approved by the authors' institutional review board or equivalent committee(s) and that board must be named by the authors in the manuscript. For research involving human participants, informed consent must have been obtained (or the reason for lack of consent explained, e.g. the data were analyzed anonymously) and all clinical investigation must have been conducted according to the principles expressed in	The tumour tissues were obtained from the Department of Dermatology, University of Debrecen, Hungary. All human studies were conducted in accordance with the principles outlined in the Declaration of Helsinki, were approved by the Regional and Institutional Ethics Committee of the University of Debrecen Medical and Health Science Centre and were conducted according to regulations (Protocol #2836-2008). Written informed consent was obtained from each patient.

the Declaration of Helsinki. Authors should submit a statement from their ethics committee or institutional review board indicating the approval of the research. We also encourage authors to submit a sample of a patient consent form and may require submission of completed forms on particular occasions. All animal work must have been conducted according to relevant national and international guidelines. In accordance with the recommendations of the Weatherall report, "The use of non-human primates in research" we specifically require authors to include details of animal welfare and steps taken to ameliorate suffering in all work involving non-human primates. The relevant guidelines followed and the committee that approved the study should be identified in the ethics statement. Please enter your ethics statement below and place the same text at the beginning of the Methods section of your manuscript (with the subheading Ethics Statement). Enter "N/A" if you do not require an ethics statement.	

From: Margit Balázs PhD, DSc
Department of Preventive Medicine, Faculty of Public Health, Medical and Health Science Center, University of Debrecen, Hungary
Kassai Str. 26/b
Debrecen 4028, Hungary
Tel: (36)-52-460-193 extension 77151
balazs.margit@sph.unideb.hu

Apr 8, 2014

Prof Robert Dante
Academic Editor
PLOS One

Dear Prof Robert Dante,

We would like to thank both Reviewers for thoroughly reviewing our manuscript. The revised version of the manuscript is being sent by a new title "*DNA methylation characteristics of primary melanomas with distinct biological behaviour".* We hope that the new title may reflect better the comprehensive analysis of our studies aiming at providing a general view in how DNA methylation associates with the distinct clinical characteristics of primary melanoma and how it accompanied by other somatic alterations. We have also answered all the comments and questions one by one.

We hope that our revised manuscript will meet the high standards of your prestigious journal.

Sincerely yours,

Prof. Margit Balázs

DNA methylation characteristics of primary melanomas with distinct biological behaviour

Szilvia Ecsedi[1, 2], Hector Hernandez-Vargas[3], Sheila C. Lima[3], Laura Vizkeleti[1, 2], Reka Toth[1], Viktoria Lazar[1],Viktoria Koroknai[1], Timea Kiss[1], Gabriella Emri[4], Zdenko Herceg[3], Roza Adany[1,2] and Margit Balazs[1, 2]

[1]Department of Preventive Medicine, Faculty of Public Health, University of Debrecen, Hungary

[2]MTA-DE- Public Health Research Group, University of Debrecen, Hungary

[3]International Agency for Research on Cancer, Section of Mechanisms of Carcinogenesis, Epigenetics Group, Lyon, France

[4]Department of Dermatology, Faculty of Medicine, University of Debrecen, Hungary

Corresponding author: Margit Balazs, Department of Preventive Medicine, Faculty of Public Health, Medical and Health Science Centre, University of Debrecen,
Debrecen 4028 Kassai út 26/b, Hungary; E-mail: balazs.margit@sph.unideb.hu

Keywords: primary melanoma, tumour progression, epigenetics, DNA methylation, hypermethylation, hypomethylation, copy number alteration, array CGH, BRAF mutation

Abstract

In melanoma, the presence of promoter related hypermethylation has previously been reported, however, no methylation-based distinction has been drawn among the diverse melanoma subtypes. Here, we investigated DNA methylation changes associated with melanoma progression and links between methylation patterns and other types of somatic alterations, including the most frequent mutations and DNA copy number changes.

Our results revealed that the methylome, presenting in early stage samples and associated with the $BRAF^{V600E}$ mutation, gradually decreased in the medium and late stages of the disease. An inverse relationship among the other predefined groups and promoter methylation was also revealed except for histologic subtype, whereas the more aggressive, nodular subtype melanomas exhibited hypermethylation as well. The Breslow thickness, which is a continuous variable, allowed for the most precise insight into how promoter methylation decreases from stage to stage. Integrating our methylation results with a high-throughput copy number alteration dataset, local correlations were detected in the MYB and EYA4 genes. With regard to the effects of DNA hypermethylation on melanoma patients' survival, correcting for clinical cofounders, only the KIT gene was associated with a lower overall survival rate.

In this study, we demonstrate the strong influence of promoter localized DNA methylation changes on melanoma initiation and show how hypermethylation decreases in melanomas associated with less favourable clinical outcomes. Furthermore, we establish the methylation pattern as part of an integrated apparatus of somatic DNA alterations.

Introduction

DNA methylation, along with covalent histone posttranslational modifications, chromatin remodelling and non-coding RNA-mediated gene interference, represents an important mechanism in the integrated apparatus of epigenetic regulation [1,2]. In addition to playing a role in several physiological processes [3,4,5], epigenetic mechanisms have been described as key factors in modifying the accessibility of DNA to transcription factors and, therefore, in altering the gene expression patterns of several cancer types [6,7,8]. Given the existence of relatively simple approaches that require even minute amounts of tumour DNA, the best factor described involved in melanoma epigenetics is DNA methylation, a covalent modification of mainly cytosines. The DNA hypermethylation is usually strictly localised to the transcriptionally active gene regions and promoters and directly inhibits gene expression. In the field of malignant melanoma epigenetics, there are substantial amounts of data available regarding gene silencing associated with the localised CpG hypermethylation of specific gene promoters. However, most of the provided data are derived from cell lines or were generated using single-gene approaches [9,10,11,12,13,14]. Despite the fact that some groups have attempted to conduct array-based experiments, to date, there are no methylation markers of the diverse melanoma subgroups based on a stratified analysis with sufficient statistical power [1]. Therefore, having chosen a powerful and high-throughput bead array technology, we performed array-based experiments to define the methylation pattern of 1,505 gene promoters. Previous studies have provided irrefutable proof of the reproducibility of this approach [6,7,15,16]. The simultaneous detection of transposonal demethylation and promoter methylation changes should provide valuable information regarding the molecular mechanisms potentially responsible for the aggressive phenotype of malignant melanoma. Recently, it has become widely accepted that Knudson's two-hit hypothesis is often confirmed through a combination of differing types of genomic alterations [17,18], which

prompted us to investigate whether methylation patterns are associated with other types of somatic alterations, such as the most frequent mutations (BRAF and NRAS) and DNA copy number (CN) alterations. Notable previous investigations demonstrated the prognostic relevance of CN aberrations [19,20,21,22]. Therefore, we also highlighted the cis-and trans-acting CN alterations of gene expression in malignant melanoma [23]. Moreover, we and others have demonstrated the association of BRAF and NRAS mutations with CN alterations using BAC arrays, suggesting a central role of BRAF mutations in gene copy number changes [21,24,25]. Additionally, a single group reported that the impact of BRAF signalling on gene methylation is widespread [26]. Despite the promising initial results, to our knowledge, no direct, array-based experiments have been performed in an integrative approach in a wide variety of primary melanomas. Therefore, we aimed to obtain better insight into how the DNA methylation changes are associated with distinct somatic alterations and contribute to melanoma progression.

Materials and Methods

Melanoma samples

Forty-two primary melanomas were included in Illumina bead assays. The clinicopathological data of the primary melanomas are summarised in Table 1.

The tumour tissues were obtained from the Department of Dermatology, University of Debrecen, Hungary. All human studies were conducted in accordance with the principles outlined in the Declaration of Helsinki, were approved by the Regional and Institutional Ethics Committee of the University of Debrecen Medical and Health Science Centre and were conducted according to regulations (Protocol #2836-2008). Written informed consent was obtained from each patient. The tumour diagnoses were made based on formalin-fixed

paraffin-embedded tissue sections using haematoxylin and eosin staining. The melanoma tumour staging was determined according to the new melanoma TNM staging system [27].

Genomic DNA and total RNA extraction

After surgical excision, the fresh tissues were immediately placed in RNA later solution (Applied Biosystems, Foster City, USA), and high-quality total RNA was prepared from the primary melanoma tissues using the RNeasy Mini Kit according to the supplier's protocol (Qiagen, GmbH, Germany). The obtained RNA concentrations were measured using a NanoDrop ND-1000 UV-Vis Spectrophotometer (Wilmington, Delaware, USA). The RNA sample integrity was determined with the Agilent 2100 Bioanalyser using the RNA 6000 Nano Kit (Agilent Technologies, Palo Alto, CA, USA). All RNA samples exhibited a 28S/18S ribosomal RNA ratio greater than 1.5.

The G-spin™ Genomic DNA Extraction Kit (Intron, Korea) was used to isolate high-molecular-weight DNA from primary melanomas according to the manufacturer's protocol. To determine the quantity of DNA obtained, we used a NanoDrop ND-1000 UV-Vis Spectrophotometer. The DNA integrity was verified via 1.2% agarose gel electrophoresis.

Bead Assay experiments

The quantitative methylation status of the 1505 CpG sites corresponding to 807 cancer-related gene promoters was determined using the Illumina GoldenGate Methylation Assay (Illumina, San Diego, CA, USA) on bisulphite-treated DNA samples corresponding to 42 primary melanomas. Bisulphite treatment was performed on 500 ng DNA using the EZ DNA Methylation-Gold Kit (Zymo Research). Duplicate samples were included to measure inter-array reproducibility for quality control. The GoldenGate assay consists of two allele-specific oligos (ASO) and two locus-specific oligos (LSO) for each CpG site. Each ASO–LSO oligo

pair corresponds to either the methylated or unmethylated state of the CpG site. Each methylation CpG spot is represented by two-color fluorescent signals from the M (methylated) and U (unmethylated) alleles. BeadStudio version 3.2 (Illumina) was used for obtaining the signal values (Avg-Beta) corresponding to the ratio of the fluorescent signal from the methylated allele (Cy5) to the sum of the fluorescents signals of both methylated (Cy5) and unmethylated alleles (Cy3), 0 corresponding to completely unmethylated sites and 1 to completely methylated sites. In agreement with the literature, 83 probes corresponding to the sex chromosomes were excluded to avoid any sex-specific bias [8]. The probes with detection P values exceeding 0.01 in more than 10% of the specimens were removed from the analyses to exclude non-biological differences. As Du et al. performed a systematic comparison between Avg-Beta values and M-values, which is the logit transformation of Avg-Beta, and M-values were proven to be statistically valid for conducting differential methylation analysis [28], M-values were used for class comparisons, whereas the raw Avg-Beta values were applied for correlation analyses (see at "Statistical Analysis").

Array CGH for studying copy number alterations

The results data of our previous Tiling Array CGH (HG18 CGH 4x72K WG Tiling v2.0) experiments (Roche NimbleGen core facility, Reykjavik, Iceland) were used which can be found under the following accession number: E-MTAB-947 (Array Express Archive repository).

The GISTIC algorithm was used to identify regions containing a statistically high frequency of copy number aberrations compared to the "background" aberration frequency. This function is most appropriate for cancer samples, as it was designed using a cancer dataset [29]. After the gain/loss aberrations were identified in each sample, a statistic (the G score) was calculated for each aberration. This G score is a measure of the frequency of occurrence

of the aberration and the magnitude of the copy number change (log ratio intensity) at each location in the aggregate of all samples in the dataset. Each location is scored separately for gains and losses. The locations in each sample are permuted, simulating data with random aberrations, and this random distribution is compared to the observed statistic to identify scores that are unlikely to occur by chance alone.

Array CGH results were verified using four colour FISH (Abott Molecular Inc., USA). The FISH experiments were performed according to the Suppliers' protocol and visualized by Zeiss Axio Imager Confocal Microscopy.

Quantitative RT-PCR

The expression status of selected genes (FGFR3, MCAM and IL8) was measured using quantitative real-time PCR with the ABI Prism® 7900HT Sequence Detection System (Applied Biosystems, Carlsbad, California, USA). Reverse transcription (RT) was carried out on total RNA (600 ng) using the High Capacity cDNA Archive Kit, according to the protocol of the supplier (Applied Biosystems, Carlsbad, California, USA). Predesigned TaqMan® Gene Expression Assays (Applied Biosystems, Carlsbad, California, USA) were used to perform qPCR for the abovementioned 3 genes.

Statistical analyses

The effect of localised methylation on clinical predictors, BRAF^{V600E} mutation and patient survival

We applied random variance t-statistics on all the binary data classes such as Breslow thickness with the cut-off value of 4 mm; metastasis, ulceration and histologic subtype. Being continuous variable, Breslow thickness can be divided into more subgroups: according to the TNM system up to 5 groups can be created, however, due to the limitation of smaller samples,

developing 3 groups based on the cut-off values of 2mm and 4mm were the most ideal. F-statistics was applied on the trichotomised Breslow groups for each CpG site.

CpG sites were considered differentially methylated when their p values based on univariate t-tests or f-tests were less than 0.01; in addition, given CpG sites were identified differentially methylated between the melanoma subgroups based on a multivariate permutation test providing 90% confidence that the false discovery rate was less than 20%. Volcano plots were applied to illustrate differential methylation patterns among clinical subgroups of melanomas (the clinicopathological characteristics of melanomas are summarized in Table 1). Volcano plots combine p-values of the t-tests for each CpG sites and ratios between the melanoma subgroups. Additionally, the trichotomised Breslow thickness groups were visualized by heatmap and compared by Principal Component Analysis (PCA).

For the aforementioned class comparisons, M-values, the logit transformations of signal intensities were used.

To evaluate the KEGG-based gene networks disturbed by DNA methylation, we applied the Efron-Tibshirani Gene Set Analysis that uses 'maxmean' statistics to identify gene sets expressed differentially among predefined classes [30]. The threshold for determining significant gene sets was 0.01 in each approach.

The Cox proportional univariate approach was performed on each gene to test whether the methylation status of a particular gene significantly influences the survival at the $p< 0.05$ level. To control for covariates on survival and to predict the survival risk, the Supervised Principal Components method was used.

As normal tissues were not involved in or studies we used external dataset from the study of Conway et al. involved 27 naevi [15] to check the methylation status of a given gene in control tissues.

Remaining statistics were performed using SPSS 19.0 and GraphPad Prism 6.0 demo version. Venn diagram was made by VENNY, an interactive tool for comparing lists with Venn Diagrams developed by Oliveros, J.C. (2007). The tool is available at: http://bioinfogp.cnb.csic.es/tools/venny/index.html.

Relationship between methylation patterns and copy number alterations

We studied how DNA copy number changes and methylation pattern associated within the same genetic loci. For this purpose, the copy number and localised methylation data of the corresponding genomic regions were simultaneously analysed gene-by-gene using CGH Tools, and Pearson's correlation was performed with $p<0.01$ after correction for multiple testing. Additionally, Fisher's exact test was applied to identify the genome sequences where gene methylation occurs frequently.

Results

Methylation patterns of melanoma subgroups

Our experimental design for applying the Illumina Bead Assay included two replicate samples among arrays to measure the inter-array reproducibility. Technical replicates were significantly correlated with each other by Pearson's correlation (Replicate #1: $r^2= 0.95$, $p<0.001$; Replicate #2: $r^2= 0.98$, $p< 0.001$).

After the initial filtering process, 895 CpG sites were available for further analyses and M-values, logistically transformed Avg-Beta values, were used for statistical approaches.

Our main goal was to investigate the relationship between the distinct biological types of melanomas and the promoter methylation levels. As the multivariate permutation test provides a tight probabilistic control on the proportion of false discoveries, this test was used for class comparison on each predefined subgroup (the clinical subgroups of primary

melanomas are detailed in Table 1) according to the following criteria: CpG sites were considered differentially methylated when their p values were less than 0.01 and FDR rates were below 0.2.

Figure 1A demonstrates that relatively large number of CpG sites was found to be differentially methylated between melanoma subgroups. Interestingly, the majority of these CpGs were characterised by decreased DNA methylation levels in samples with poor prognosis (larger than 4 mm, metastatic, ulcerated and nodular primary melanomas). Histologic subtype exhibited a more disturbed methylation pattern involving high number of differentially methylated genes in both superficial and nodular subtype. As it can be seen in Figure 1A, some of the differentially methylated individual genes were represented by more than one significant CpG sites arguing in favour of the consistency of given alterations. Altogether, 111 differentially methylated genes were identified in the context of aforementioned clinical predictors: 43 individual genes were hypermethylated and 68 genes hypomethylated in melanomas with less favourable clinical outcome. The differentially methylated gene lists specific for the Breslow thickness, ulceration, metastatic capacity and histologic subtype are detailed in Supplementary Table 1. Venn diagrams (Figure 1B) indicate the common properties among genes with decreased and increased DNA methylation, respectively.

Being a continuous variable, Breslow thickness allowed the most precise insight into how methylation pattern changes across melanoma stages. In Figure 2A, the heatmap horizontally shows the primary melanoma samples with distinct Breslow thicknesses. The intensive hypermethylation of 45 CpGs is marked with brown colour in the early stage tumours (Breslow thickness < 2mm), and this hypermethylation decreases during the medium and advanced stages. Low-level methylation values are represented with yellow colour. In other types of cancer, hypermethylation has been shown to be associated with tumour progression.

Interestingly, the hypermethylation patterns of 45 CpGs, which are detected in the early stages of melanomas, gradually decrease in the medium stages and almost disappear in late stages of the disease. The Principal Component Analysis (Figure 2B) clearly demonstrated that, according to the pattern of the 45 hypermethylated CpGs, the melanoma groups were significantly separated.

It is important to note that normal tissues were not used in our experiments. However, such datasets can be found in the literature, and we were therefore able to correct for the methylation status of normal naevi specimens (see Materials and Methods). These results thus argue that the hypermethylation of the 45 CpGs occurs early, in melanomas less than 2 mm, and then decreases during melanoma progression.

In addition to individual gene signatures, we aimed to determine whether the perturbed KEGG-based gene networks are related to localised methylation patterns. We identified differentially methylated genes belongs to Cell cycle pathways in primary melanomas with metastatic capacity. Genes associated at Leukocyte signalling were also demonstrated to be differentially methylated in ulcerated samples (Figure 3A). Interestingly, Cell communication and ECM-receptor interaction networks were found to be significant at the 0.01 level between $BRAF^{V600E}$ mutant and wild type samples, notwithstanding the fact that, we were unable to find differentially methylated CpGs at the individual gene level (Figure 3A-B). The full list of CpG probes is given in Supplementary Table 2. There was poor overlap (Figure 3C) between the differentially methylated genes associated with $BRAF^{V600E}$ mutation and clinical subgroups discussed above.

Our analysis of the effects of hypermethylation on patient survival identified an association between six hypermethylated genes (DSP, EPHB6, HCK, IL18, IRAK3 and KIT) with lower OS values. Four of the six genes (DSP, HCK, IL18 and KIT) exhibited significantly different Kaplan-Meier curves (Figure 4). However, when we included patient age, gender and

$BRAF^{V600E}$ mutation status in the survival risk prediction model, only the KIT gene remained significant.

Analysis of the mRNA expression level of the differentially methylated genes identified in melanoma

Three genes among the differentially methylated panel were chosen to measure mRNA expression levels by qPCR (FGFR3, MCAM and IL8) according to the following selection criteria: we exclusively focused on genes that had not been previously referred to as methylated in melanomas; furthermore, FGFR3 was chosen in the context of histologic subtype and MCAM of Breslow thickness, while IL8, being a commonly methylated gene among distinct clinical groups was measured across in all categories (Breslow thickness, histologic subtype, ulceration and metastatic capacity).

Inverse relationships were found between hypermethylation and mRNA expression regarding FGFR3, MCAM and IL8 as well, supporting the notion that the methylation pattern are functionally relevant to gene expression. Significant ($p<0.05$) MCAM mRNA expression level differences were revealed between smaller (Breslow thickness $\leq$ 4mm) and larger (Breslow thickness > 4mm) melanomas. IL8 expression differed as well between sample distinct categories of Breslow thickness, melanoma surface ulceration and metastatic capacity. The qPCR and corresponding correlation results are summarised in Figure 5.

Coincidence of localised hypermethylation and copy number alterations

We determined the frequent copy number gains and losses associated with the $BRAF^{V600E}$ mutation (Figure 6A) and Breslow thickness (Supplementary Table 3) in primary melanomas. As expected, a set of marked copy number alterations was associated with both the $BRAF^{V600E}$ (Figure 6A) mutation and Breslow thickness (Supplementary Table 3) categories.

In the $BRAF^{V600E}$ mutant samples, significant CN losses (Figure 6B) were found at in the 1p, 1q, 2p, 4q, 6q, 7p, 9p, 9q, 10p, 10q, 11p, 14p, 15p, 17p, 20p and 21p regions, whereas CN gains (Figure 6C) were detected across chromosomes 1q, 6p, 7p, 7q, 8q, 11q, 15q, 20q and 22q.

In the late stages of primary melanomas (Breslow thickness > 4mm), significant CN losses were observed more frequently and comprised deletions of 1p, 4q, 7p, 9p, 14p and 21p, whereas CN gains were only observed in the 11q region, as summarised in Supplementary Table 3. Despite not reaching a significant level, it is worth noting that the CN losses in 19p12 (harbouring the DNA Methyltransferase-1 gene) were exclusively associated with more advanced stages (Breslow thickness > 2mm; Supplementary Figure 1A). However, among the late-stage samples (Breslow thickness > 4mm), CN gains were also found with CN losses in some samples. Supplementary Figure 1B-D represents late-stage melanomas that exhibited CN losses in 19p12.

In addition to the general mapping of the CN-altered genomic regions, we quantitatively assessed the coincidence of CN alteration and methylation patterns gene by gene. Similar to other studies, we established gene level measurements by averaging the methylation states within gene-specific regions. As significantly and positively correlated genes were revealed at the levels of methylation and CN alteration, the correlations cannot possibly represent coordinated allele loss and hypermethylation; nevertheless, these results do not remain significant after the multiple correction procedure. Moreover, direct correlation often involves genome parts that are positively correlated at the level of methylation and CN without detected CN changes or altered methylation. Therefore, we applied an alternative approach based on the frequency of methylated genes harbouring significant CN alterations to test Knudson's two-hit hypothesis. As indicated in Figure 6A, 6q12-6q25.1 comprises a relatively large, significant CN loss and two hypermethylated genes, namely, EYA4 (6q23) and MYB

(6q22-q23). When measured quantitatively, a significant inverse correlation was observed between CN loss and DNA hypermethylation (Figure 6 D-E).

Array CGH results were further confirmed by four colour FISH experiments specific for 11q13 (specific for CCND1 gene), 6p25 (specific for RREB1 gene), 6q23 (specific for MYB gene) and centromere 6 on 27 primary melanomas (Figure 7A-C).

Discussion

Among epigenetic aberrations, DNA methylation itself features a diverse presence [31]. Recently, 5-hydroxymethylcytosine (5-hmC) has been identified as a constituent of mammalian DNA and described as the sixth base of the genome [32]. The loss of 5-hmC has been highlighted as a hallmark of melanoma by a single, remarkable study, whereas interesting clues as to the role of 5-hydroxymethylcytosine are still emerging [33]. In contrast to 5-hmC, the importance of 5-methylcytosine (5-mC) in cancer cells is much more firmly established [1,34]. Aberrant promoter DNA hypermethylation or localised methylation preferably occurs in CpG dinucleotide-dense regions, resulting in the down-regulation of the corresponding gene [1,14].

It has recently become apparent that malignant melanomas feature hypermethylation, and currently more than 80 genes – mainly in promoter regions – are hypermethylated at a single-gene level [1,12,31]. Taking a global view of the available data, the number of primary tumour samples involved in the studies and the frequency of positive results do not allow determining whether the hypermethylated genes described are appropriate for diagnosis or can be considered candidate therapeutic targets. Moreover, most of the data provided are derived from cell lines and estimated methylation values indirectly consisting of three steps: measuring mRNA or protein expression in cell lines, treating samples with a specific drug that acts against the process of methylation and measuring gene expression again. Nonetheless,

powerful arguments have been presented in the literature that support direct experiments being less ambiguous; furthermore, most of the groups conducting direct measurements have applied candidate gene approaches [31,35].

In addition to the rapid progress that has been made in studying promoter hypermethylation at the single-gene level, only two groups have attempted to conduct array-based experiments to identify the methylation pattern of thousands of gene promoters [15,36]. Regrettably, one group has focused only on comparing the methylation level of primary invasive melanomas with benign melanocytes and has clearly identified a group of genes in a statistically powerful interpretation that can be used to discriminate naevi from melanomas based on their methylation signature [15]. Another group has examined the short-term cultures of homogeneous stage III specimens [36].

As no data are currently available regarding the methylation markers of diverse melanomas with different clinical behaviours, we performed a systematic comparison of localised methylation patterns among 42 primary melanomas using the Illumina Golden Gate Cancer Panel Bead Assay. We found 111 differentially methylated CpGs altogether among melanoma subgroups and the majority of CpG sites were hypermethylated in melanomas that represent more favourable prognoses including a non-ulcerated tumour surface, superficial spreading histological subtype, non-metastatic subgroup and smaller tumour thickness (Breslow thickness < 2 mm). Regarding more advanced-stage specimens, the hypermethylome detected in melanomas that represents better prognoses markedly decreased. The decrease in the methylation levels occurred gradually, as the continuous Breslow thickness variables allowed us to distinguish more than two groups among primary melanomas and to map the progress of demethylation during distinct stages (Breslow thickness < 2 mm; Breslow thickness 2 - 4 mm; Breslow thickness > 4 mm). The genes involved in demethylation partially overlap among clinical subgroups: five genes (EMR3, SEPT9, IL8, MMP14 and SLC22A18) were found to

be commonly demethylated in large (Breslow thickness > 4 mm), nodular subtype, ulcerated and metastatic melanomas. The SEPT9 gene is an ovarian tumour suppressor playing a role in cell cycle control [37]; IL8 gene expression is elevated in metastatic melanomas and can increase the level of MMP2 [38]; SLC22A18 has been reported to be down-regulated due to promoter hypermethylation in gliomas [38,39]; MMP14 has not been found to play a role in melanoma progression thus far. Among the aforementioned clinical groups, the largest similarity (27 overlapping genes) has been detected between the demethylated genes associated with Breslow thickness and ulceration. The histologic subtype represents the most unique methylation pattern, comprising 30 differentially methylated genes between superficial and nodular melanomas.

Our results contrast those of studies describing the hypermethylation patterns of specific genes as tumour progression-related markers based on single gene approaches. However, Conway et al. supported the claim that a covalent change from cytosine to 5-methylcytosine in the promoter region occurs as an early aberration event in melanomas [15]. Notwithstanding, their results highlighted not only the hypermethylated but also the demethylated genes in heterogeneous melanomas compared to naevi. This group reported a lack of similarity – involving only two genes, namely, RUNX3 and SYK – with the previously published data.

Previously, a group published two independent studies regarding in vitro data that demonstrated how the $BRAF^{V600E}$ mutation causes widespread alterations in DNA methylation [26,40]. Along with Hou et al., we found hypermethylated CpGs accompanied by the $BRAF^{V600E}$ mutation in primary melanomas. In agreement with these observations, we also found distinct methylation pattern in $BRAF^{V600E}$ mutant primary melanomas involving genes of Cell Communication and ECM-receptor interaction networks. A similar association between the $BRAF^{V600E}$ mutation and DNA methylation was described in colon cancer, as

methylated samples convincingly represented a distinct subset encompassing almost all cases of tumours with the $BRAF^{V600E}$ mutation [41]. A remarkable study performed by Roon et al. revealed the $BRAF^{V600E}$ mutation-specific hypermethylation of CpG regions in colon cancer samples by Differential Methylation Hybridization on high-density oligonucleotide microarrays [42]. Interestingly, the authors identified several cancer-related pathways, including the PI3 kinase and Wnt signalling pathways being differentially methylated between $BRAF^{V600E}$ mutant and wild type samples. Additionally, the group found the silencing of *FOXD3 hypermethylated manner*. Based on these studies, authors suggest that a specific epigenetic pattern can contribute to a favourable context for the acquisition of $BRAF^{V600E}$ mutations [42]. However, further studies are warranted to further clarify the relationship between the mutation and DNA methylation.

In addition to the common mutations, specific patterns of CN alterations have been reported in melanomas characteristic of unfavourable clinical outcomes [21]. Furthermore, it has become obvious that $BRAF^{V600E}$ mutated melanomas display distinct patterns for CN changes, providing the first line of evidence in support of Knudson's two-hit hypothesis [19,21]. However, none of the published studies attempted to evaluate the relationship between CN alterations and DNA methylation in melanomas. Our group performed a Tiling Array CGH, and, apart from highlighting common CN losses and amplification in the subgroups of primary melanomas, we demonstrated that 6q12-6q25.1 comprises a remarkable CN loss, harbouring two hypermethylated genes on 6q23, EYA4 and MYB1. This result was measured and verified quantitatively and provides evidence for Knudson's two-hit hypothesis at the level of CN loss and DNA hypermethylation. Notably, MYB1 is an important discriminator between melanomas and naevi, as validated by FISH in 123 melanomas and 110 naevi [43,44]. The copy number deletion of MYB1 is currently used in the diagnosis of melanoma.

Our Tiling Array CGH experiments showed another important feature: the CN alterations of chromosome 19 were only detected in advanced staged primary melanomas. Notably, the altered genomic regions encompass 19p13.2, which harbours the DNMT1 gene (DNA Methyltransferase-1), which plays a role in the establishment and regulation of tissue-specific patterns of methylated cytosine residues [31]. The DNA CN alterations of DNMT1 in advanced stages primary melanomas raise crucial questions: Is demethylation, contributing to clinical outcomes, only a passive consequence of CN loss? Or do CN alterations – as was demonstrated in the context of epigenetic mechanisms and the $BRAF^{V600E}$ mutation – directly control the DNA methylation changes to influence the gene expression patterns of given molecules? Regardless of the reason for changes in methylation, we obtained better insight into how gene expression levels are regulated by DNA methylation: demethylation was associated with increased mRNA levels, whereas hypermethylation was associated with decreased levels.

In summary, we demonstrated the strong influence of DNA methylation changes on melanoma progression. However, hypermethylation, which has been greatly emphasised in the literature, appears to represent more complexity both in melanoma initiation and progression. Additionally, the inhibition of promoter hypermethylation might represent the most promising therapeutic target for the treatment of melanoma, and several types of DNMT inhibitors are currently being developed [35]. Considering the dual role of DNA methylation, further efforts are needed to investigate the importance of such drugs in melanoma treatment.

Acknowledgments

DNA methylation date analyses were performed using BRB-ArrayTools developed by Dr. Richard Simon and BRB-Array Tools Development Team. We thank Orsolya Papp for the assistance of microscopic analysis of the FISH experiments.

References

1. van den Hurk K, Niessen HE, Veeck J, van den Oord JJ, van Steensel MA, et al. (2012) Genetics and epigenetics of cutaneous malignant melanoma: a concert out of tune. Biochim Biophys Acta 1826: 89-102.
2. Heyn H, Esteller M (2012) DNA methylation profiling in the clinic: applications and challenges. Nat Rev Genet 13: 679-692.
3. Wild L, Flanagan JM (2010) Genome-wide hypomethylation in cancer may be a passive consequence of transformation. Biochim Biophys Acta 1806: 50-57.
4. James SJ, Pogribny IP, Pogribna M, Miller BJ, Jernigan S, et al. (2003) Mechanisms of DNA damage, DNA hypomethylation, and tumor progression in the folate/methyl-deficient rat model of hepatocarcinogenesis. J Nutr 133: 3740S-3747S.
5. Acquaviva L, Szekvolgyi L, Dichtl B, Dichtl BS, de La Roche Saint Andre C, et al. (2013) The COMPASS subunit Spp1 links histone methylation to initiation of meiotic recombination. Science 339: 215-218.
6. Hernandez-Vargas H, Ouzounova M, Le Calvez-Kelm F, Lambert MP, McKay-Chopin S, et al. (2011) Methylome analysis reveals Jak-STAT pathway deregulation in putative breast cancer stem cells. Epigenetics 6: 428-439.
7. Lima SC, Hernandez-Vargas H, Simao T, Durand G, Kruel CD, et al. (2011) Identification of a DNA methylome signature of esophageal squamous cell carcinoma and potential epigenetic biomarkers. Epigenetics 6: 1217-1227.
8. Hernandez-Vargas H, Lambert MP, Le Calvez-Kelm F, Gouysse G, McKay-Chopin S, et al. (2010) Hepatocellular carcinoma displays distinct DNA methylation signatures with potential as clinical predictors. PLoS One 5: e9749.
9. Furuta J, Umebayashi Y, Miyamoto K, Kikuchi K, Otsuka F, et al. (2004) Promoter methylation profiling of 30 genes in human malignant melanoma. Cancer Sci 95: 962-968.
10. Marini A, Mirmohammadsadegh A, Nambiar S, Gustrau A, Ruzicka T, et al. (2006) Epigenetic inactivation of tumor suppressor genes in serum of patients with cutaneous melanoma. J Invest Dermatol 126: 422-431.
11. Mori T, Martinez SR, O'Day SJ, Morton DL, Umetani N, et al. (2006) Estrogen receptor-alpha methylation predicts melanoma progression. Cancer Res 66: 6692-6698.
12. Liu S, Ren S, Howell P, Fodstad O, Riker AI (2008) Identification of novel epigenetically modified genes in human melanoma via promoter methylation gene profiling. Pigment Cell Melanoma Res 21: 545-558.
13. Lahtz C, Stranzenbach R, Fiedler E, Helmbold P, Dammann RH (2010) Methylation of PTEN as a prognostic factor in malignant melanoma of the skin. J Invest Dermatol 130: 620-622.
14. Sigalotti L, Covre A, Fratta E, Parisi G, Colizzi F, et al. (2010) Epigenetics of human cutaneous melanoma: setting the stage for new therapeutic strategies. J Transl Med 8: 56.
15. Conway K, Edmiston SN, Khondker ZS, Groben PA, Zhou X, et al. (2011) DNA-methylation profiling distinguishes malignant melanomas from benign nevi. Pigment Cell Melanoma Res 24: 352-360.
16. Bibikova M, Le J, Barnes B, Saedinia-Melnyk S, Zhou L, et al. (2009) Genome-wide DNA methylation profiling using Infinium(R) assay. Epigenomics 1: 177-200.
17. Houseman EA, Christensen BC, Karagas MR, Wrensch MR, Nelson HH, et al. (2009) Copy number variation has little impact on bead-array-based measures of DNA methylation. Bioinformatics 25: 1999-2005.

18. Christensen BC, Houseman EA, Poage GM, Godleski JJ, Bueno R, et al. (2010) Integrated profiling reveals a global correlation between epigenetic and genetic alterations in mesothelioma. Cancer Res 70: 5686-5694.
19. Rose AE, Poliseno L, Wang J, Clark M, Pearlman A, et al. (2011) Integrative genomics identifies molecular alterations that challenge the linear model of melanoma progression. Cancer Res 71: 2561-2571.
20. Berger MF, Garraway LA (2009) Applications of genomics in melanoma oncogene discovery. Hematol Oncol Clin North Am 23: 397-414, vii.
21. Lazar V, Ecsedi S, Vizkeleti L, Rakosy Z, Boross G, et al. (2012) Marked genetic differences between BRAF and NRAS mutated primary melanomas as revealed by array comparative genomic hybridization. Melanoma Res 22: 202-214.
22. Vizkeleti L, Ecsedi S, Rakosy Z, Orosz A, Lazar V, et al. (2012) The role of CCND1 alterations during the progression of cutaneous malignant melanoma. Tumour Biol 33: 2189-2199.
23. Rakosy Z, Ecsedi S, Toth R, Vizkeleti L, Herandez-Vargas H, et al. (2013) Integrative genomics identifies gene signature associated with melanoma ulceration. PLoS One 8: e54958.
24. Thomas NE (2006) BRAF somatic mutations in malignant melanoma and melanocytic naevi. Melanoma Res 16: 97-103.
25. Greshock J, Nathanson K, Medina A, Ward MR, Herlyn M, et al. (2009) Distinct patterns of DNA copy number alterations associate with BRAF mutations in melanomas and melanoma-derived cell lines. Genes Chromosomes Cancer 48: 419-428.
26. Hou P, Liu D, Dong J, Xing M (2012) The BRAF(V600E) causes widespread alterations in gene methylation in the genome of melanoma cells. Cell Cycle 11: 286-295.
27. Gershenwald JE, Soong SJ, Balch CM (2010) 2010 TNM staging system for cutaneous melanoma...and beyond. Ann Surg Oncol 17: 1475-1477.
28. Du P, Zhang X, Huang CC, Jafari N, Kibbe WA, et al. (2010) Comparison of Beta-value and M-value methods for quantifying methylation levels by microarray analysis. BMC Bioinformatics 11: 587.
29. Beroukhim R, Getz G, Nghiemphu L, Barretina J, Hsueh T, et al. (2007) Assessing the significance of chromosomal aberrations in cancer: methodology and application to glioma. Proc Natl Acad Sci U S A 104: 20007-20012.
30. Tibshirani R, Hastie T, Narasimhan B, Chu G (2002) Diagnosis of multiple cancer types by shrunken centroids of gene expression. Proc Natl Acad Sci U S A 99: 6567-6572.
31. Balazs M, Ecsedi, S., Vizkeleti, L., Begany, A., (2011) Genomics of human malignant melanoma. In: Tanaka IY, editor. Breakthroughs in melanoma research. Rijeka: InTech. pp. pp. 237-263.
32. Song CX, He C (2011) The hunt for 5-hydroxymethylcytosine: the sixth base. Epigenomics 3: 521-523.
33. Lian CG, Xu Y, Ceol C, Wu F, Larson A, et al. (2012) Loss of 5-hydroxymethylcytosine is an epigenetic hallmark of melanoma. Cell 150: 1135-1146.
34. Tellez CS, Shen L, Estecio MR, Jelinek J, Gershenwald JE, et al. (2009) CpG island methylation profiling in human melanoma cell lines. Melanoma Res 19: 146-155.
35. Adjemian JZ, Howell J, Holzbauer S, Harris J, Recuenco S, et al. (2009) A clustering of immune-mediated polyradiculoneuropathy among swine abattoir workers exposed to aerosolized porcine brains, Indiana, United States. Int J Occup Environ Health 15: 331-338.
36. Sigalotti L, Covre A, Fratta E, Parisi G, Sonego P, et al. (2012) Whole genome methylation profiles as independent markers of survival in stage IIIC melanoma patients. J Transl Med 10: 185.

37. Scott M, McCluggage WG, Hillan KJ, Hall PA, Russell SE (2006) Altered patterns of transcription of the septin gene, SEPT9, in ovarian tumorigenesis. Int J Cancer 118: 1325-1329.
38. Zhang H, Fu T, McGettigan S, Kumar S, Liu S, et al. (2011) IL8 and Cathepsin B as Melanoma Serum Biomarkers. Int J Mol Sci 12: 1505-1518.
39. Chu SH, Feng DF, Ma YB, Zhang H, Zhu ZA, et al. (2011) Promoter methylation and downregulation of SLC22A18 are associated with the development and progression of human glioma. J Transl Med 9: 156.
40. Liu D, Liu X, Xing M (2012) Epigenetic genes regulated by the BRAFV600E signaling are associated with alterations in the methylation and expression of tumor suppressor genes and patient survival in melanoma. Biochem Biophys Res Commun 425: 45-50.
41. Bae JM, Kim JH, Kang GH (2013) Epigenetic alterations in colorectal cancer: the CpG island methylator phenotype. Histol Histopathol.
42. van Roon EH, Boot A, Dihal AA, Ernst RF, van Wezel T, et al. (2013) BRAF mutation-specific promoter methylation of FOX genes in colorectal cancer. Clin Epigenetics 5: 2.
43. Senetta R, Paglierani M, Massi D (2012) Fluorescence in-situ hybridization analysis for melanoma diagnosis. Histopathology 60: 706-714.
44. Gerami P, Li G, Pouryazdanparast P, Blondin B, Beilfuss B, et al. (2012) A highly specific and discriminatory FISH assay for distinguishing between benign and malignant melanocytic neoplasms. Am J Surg Pathol 36: 808-817.

Figure legends

Figure 1 Methylation patterns of primary melanomas associated with known clinical predictors

(A) Volcano plots of differentially methylated genes associated with known predictors. Blue dots indicates decreased and red indicates increased methylation as follows: Breslow thickness: 51 hypomethylated probes (43 individual genes) and 5 hypermethylated probes (5 individual genes); metastatic capacity: 23 hypomethylated probes (21 individual genes) and 5 hypermethylated probes (4 individual genes), ulceration: 48 hypomethylated probes (43 individual genes) and 8 hypomethylated probes (8 individual genes), histologic subtype: 28 hypomethylated probes (26 individual genes) 23 hypermethylated probes (20 individual genes) **(B)** A Venn diagrams indicate the overlap of differentially methylated genes (in left: number of hypomethylated genes; in right: number of hypermethylated genes) for each clinical predictor class.

Figure 2 Hypermethylation is an early event in melanomas and decreases with tumour thickness

(A) The heatmap demonstrates the hypermethylation patterns (indicated in brown colour) of 45 CpGs, which can be detected in the early stages of melanomas (horizontal purple colour) but decrease from the medium stage (horizontal green colour) to the late stage (horizontal blue colour). **(B)** The principal component analysis for the distinction of the Breslow thickness the sample groups (large: blue dots; medium: green dots; and small melanoma samples: purple dots) based on the 45 differentially methylated CpGs. The analysis revealed that, according to the first three components, which covered the 56% of the total variance, the three groups were significantly different ($p < 0.05$)

Figure 3 Differentially methylated gene sets between the $BRAF^{V600E}$ mutant and wild-type classes

(A) Differentially methylated gene sets between $BRAF^{V600E}$ mutant and wild-type, metastatic and non-metastatic, ulcerated and non-ulcerated classes according to the Kyoto Encyclopaedia of Genes and Genomes. **(B)** Average log-ratios of methylation intensities in $BRAF^{V600E}$ mutant and wild-type melanomas. Red indicates significant genes associated with ECM-receptor interaction and blue depicts significant genes on Cell communication pathway.

(Eleven genes overlap between the ECM-receptor interaction and Cell communication.) **(C)** Venn diagram shows lack of overlap between differentially methylated genes associated with $BRAF^{V600E}$ mutation and the known clinical predictors as Breslow thickness, metastatic capacity, ulceration and histologic subtype.

Figure 4 Hypermethylated genes associated with decreased survival rate in melanoma patients

The Kaplan-Meier curves for genes (DSP, EPHB6, HCK, IL18, IRAK3 and KIT) whose hypermethylation was associated with a lower overall survival rate (OS); the Cox proportional univariate approach was performed on each gene to test whether a methylation status of a particular gene significantly influences the survival at the $p < 0.05$ level.

Figure 5 Relationship between gene expression and DNA methylation

The gene expressions of MCAM, FGFR3 and IL8 were measured by qRT-PCR and are presented as bars (fold change in left Y axis), and Avg-Beta methylation values are demonstrated as lines (shown in right Y axis). Methylation data was extracted from Illumina bead assay, with distinct probes represented as different lines. Gene expression differences among the groups were analysed using the Mann-Whitney test, which revealed significant differences for the MCAM and IL8 genes.

Figure 6 Coincidence of DNA copy number (CN) alterations and hypermethylation

(A) The distribution of CN aberrations (red indicates CN losses and blue indicates CN gains on the frequency plot) specific for the $BRAF^{V600E}$ mutant (purple line on the left) and $BRAF^{V600E}$ wild-type (green line on the left) primary melanomas. The methylated genes are shown as blue lines in the lower part of the figure, and the red dotted circle highlights 6q23 as the only region where a coincidence was revealed. The significant CN alterations are highlighted in grey in the upper part of the figure. Frequent CN losses **(B)** and CN gains **(C)** are given based on the G-score of GISTIC algorithm, which is a measure of the frequency of occurrence of the aberration and the magnitude of the CN alteration at each location in the aggregate of all samples in the dataset. The locations of the alterations in each sample are permuted, simulating data with random aberrations, and the significance is represented as Q-Bounds. Grey lines indicate the peak, whereas the grey shaded area is an extended peak based on leave-one-out algorithm to allow for errors in the boundaries in a single sample. **(C)**

Correlation plot for CN alterations and DNA methylation regarding the MYB gene and **(D)** the EYA4 gene.

Figure 7 FISH analysis to confirm array CGH results

CN alteration at specific regions of a representative $BRAF^{V600E}$ mutant primary melanoma: **(A)** CN gains were revealed at chromosome 6p while CN losses occurred at chromosome 6q in $BRAF^{V600E}$ samples. **(B)** High level CN gain was seen at the region of 11q13-q14. **(C)** Four colour FISH was performed to verify the CN altered genomic regions: green fluorescence (gain of CCND1 gene on 11q13), yellow fluorescence (loss of MYB gene on 6q23), red fluorescence (gain of RREB1 gene on 6p25), whereas blue fluorescence indicates centromere 6.

Supplementary Figure 1 Copy number alteration of chromosome 19 in Breslow thickness > 4 mm melanomas

(A) The Tiling Array CGH revealed characteristic CN differences among the three sample groups (pink line on the left: Breslow thickness < 2mm; yellow line: Breslow thickness 2 – 4 mm; red line: Breslow thickness > 4 mm) regarding the CN alterations of chromosome 19. The CN-altered regions involve 19p13.2 harbouring the Methyltransferase-1 gene (DNMT1). Panels **(B-E)** depict representative figures of CN losses revealed exclusively in medium- or advanced-stage (according to Breslow thickness) primary melanomas.

Table 1. Clinical-pathological parameters of primary melanomas

Variables	No. of tumours analysed by Illumina bead assay
All patients	42
Histological subtype	
SSM[1]	26
NM[2]	16
Gender	
Female	20
Male	22
Age (years)	
20-50	14
≥50	28
Breslow thickness (mm)[3]	
≤4	26
>4	16
Breslow thickness (mm)[4]	
≤2	15
2-4	11
>4	16
Location of primary tumour	
Extremity	21
Trunk	20
Head	1
Metastasis formation[5]	
Absent	20
Present	22
Patient's survival[6]	
Alive	21
Exitus	21
Ulceration	
Absent	20
Present	22
$BRAF^{V600E}$ mutation	
$BRAF^{V600E}$ mutant	12
$BRAF^{V600E}$ wild type	24

[1]Superficial spreading melanoma.[2]Nodular melanoma.[3]Thickness categories are based on the current staging system. [4]Thickness categories are based on the current staging system.[5]Metastasis of the examined primary tumours. [6]Patients with at least a 5-year follow-up period were included.

Figure_1
Click here to download high resolution image

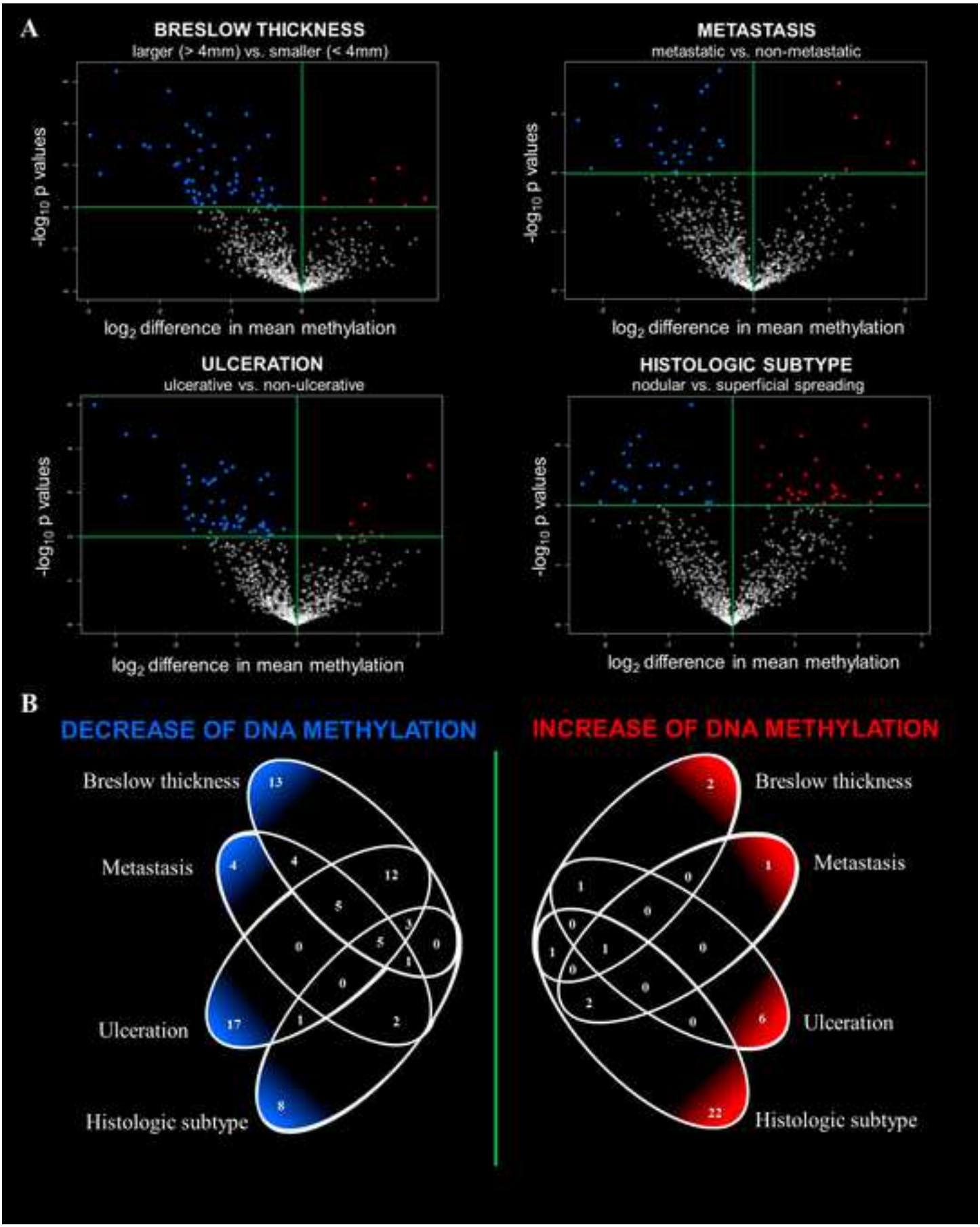

Figure_2
Click here to download high resolution image

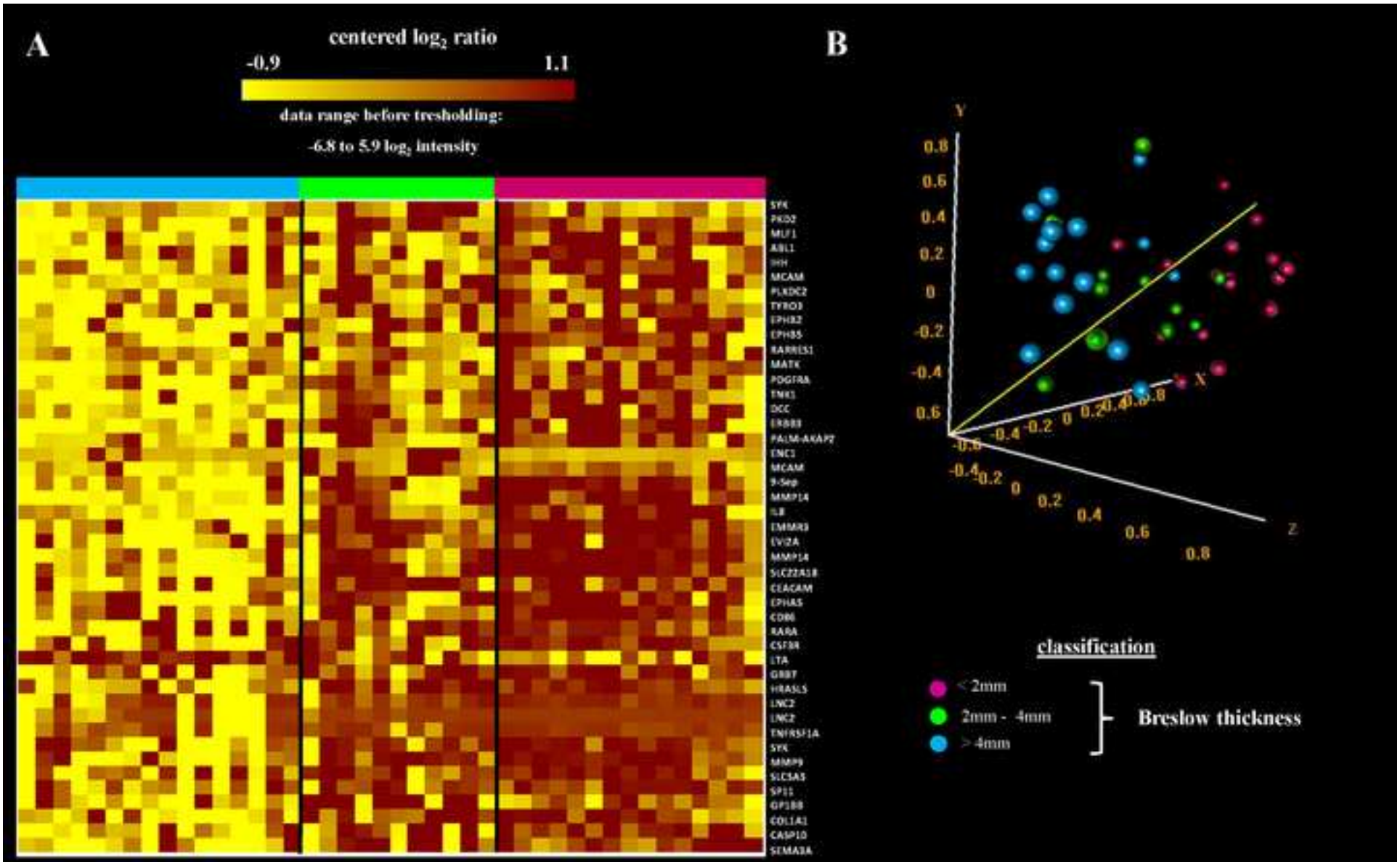

Figure_3
Click here to download high resolution image

A

Characteristics	KEGG Pathway	Pathway description	No. of CpG probes	No. of individual genes	p-value (Efron-Tibshirani GSA test)
$BRAF^{V600E}$ mutation	hsa01430	Cell communication	21	14	< 0.005
	hsa04512	ECM-receptor interaction	17	13	0.005
Metastatic capacity	hsa04110	Cell cycle	26	24	< 0.005
Ulceration	hsa04670	Leukocyte transendothelial migration	22	17	0.005

B

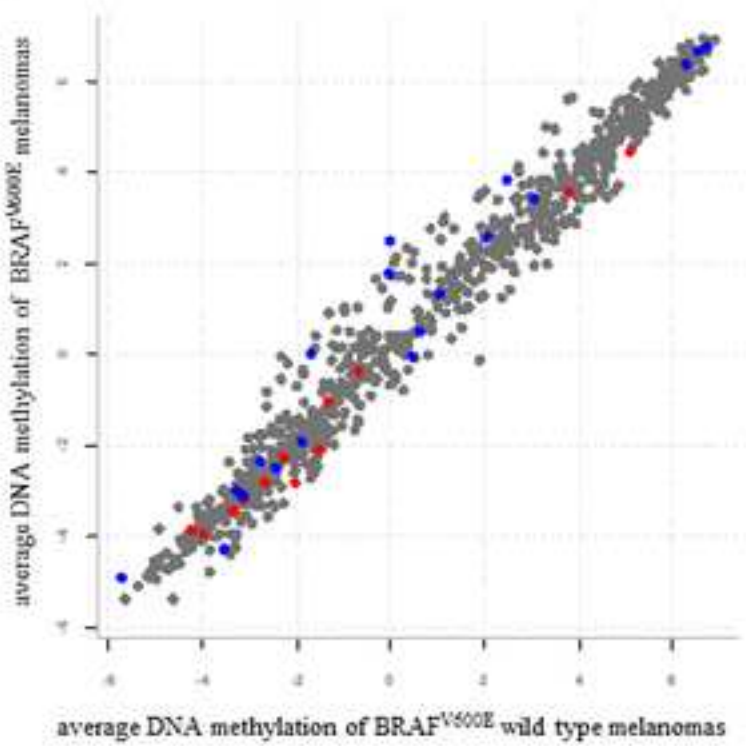

C

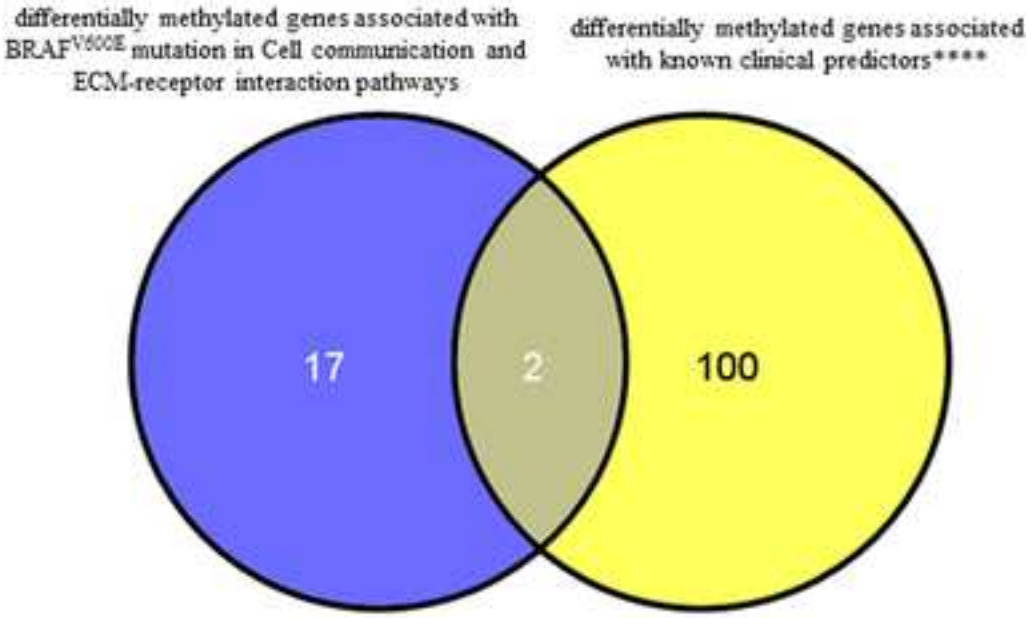

Figure_4
Click here to download high resolution image

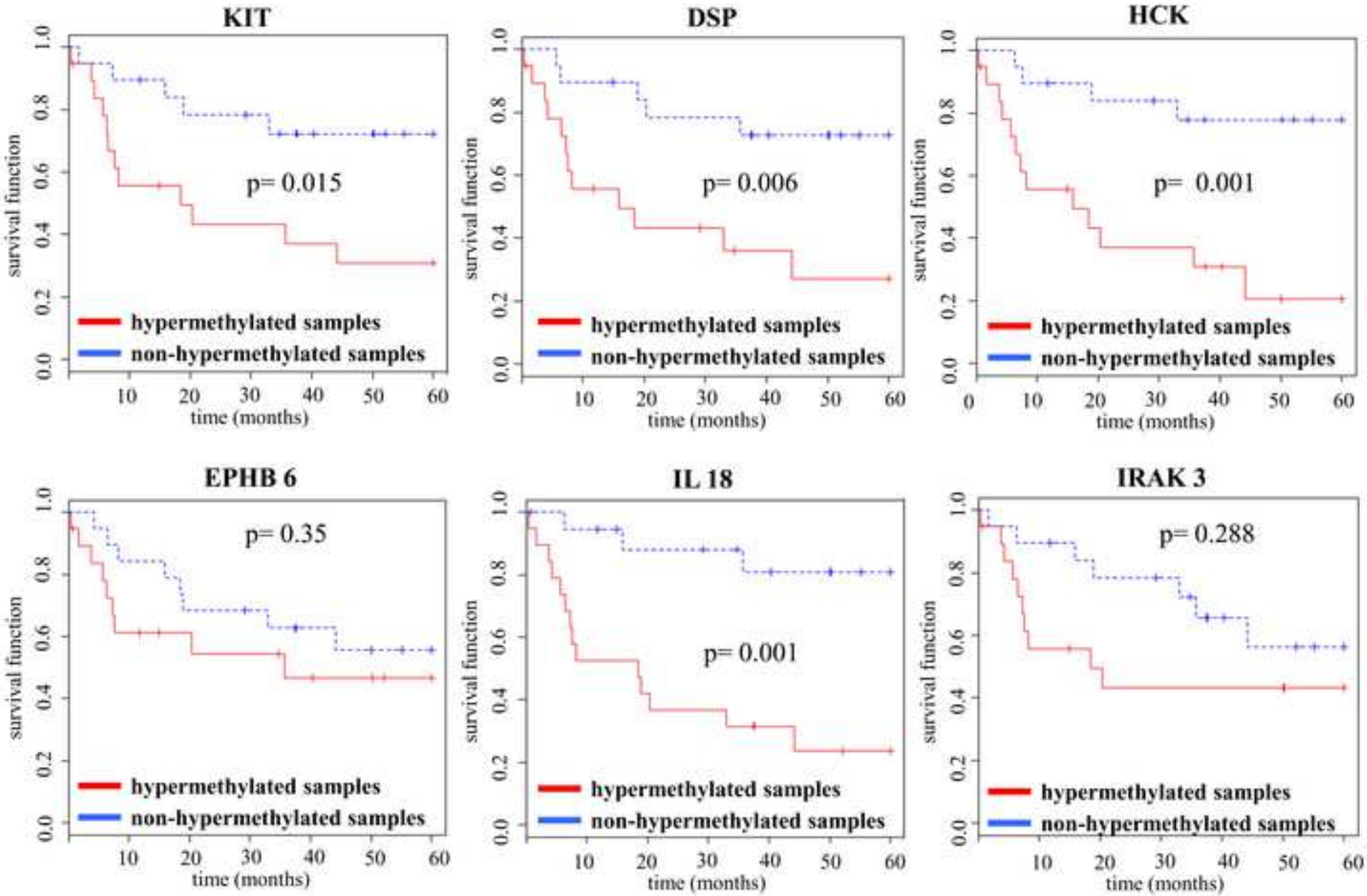

Figure_5
Click here to download high resolution image

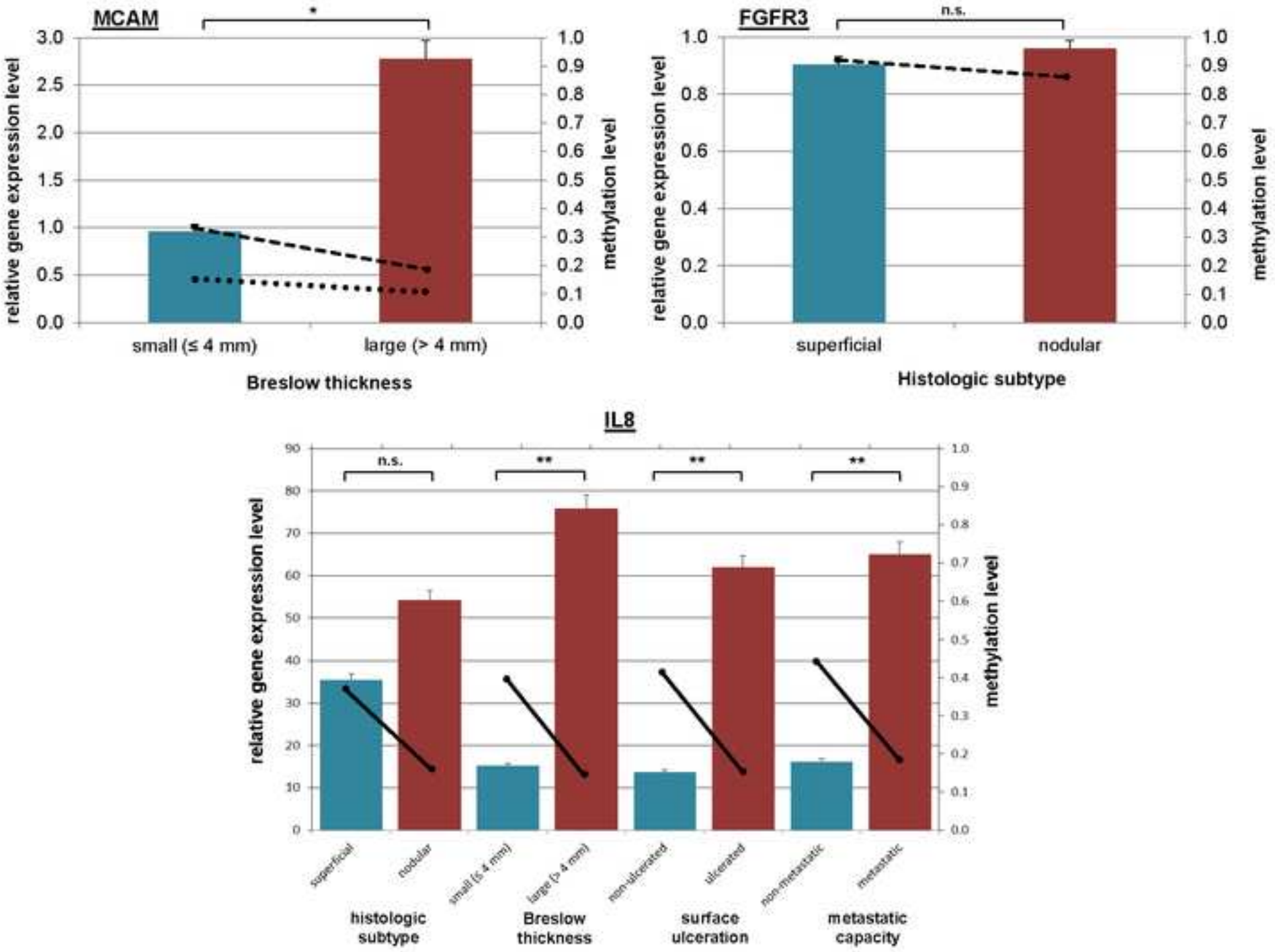

Figure_6
Click here to download high resolution image

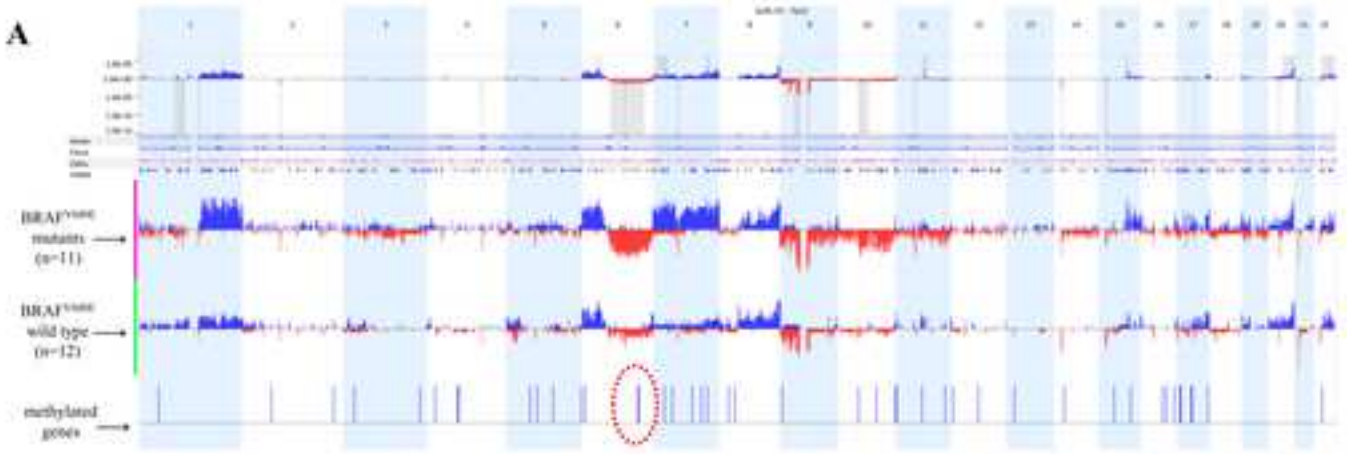

B

Frequent copy number losses associated with BRAF^{V600E} mutation

Genomic Region	Q-Bound	G-Score
chr1:84,589,102-109,787,706	0.034	3.41
chr1:141,494,294-142,396,987	0.039	3.21
chr2:91,050,524-91,508,588	0.013	3.89
chr4:132,814,794-133,128,048	<0.001	5.11
chr6:69,111,856-150,228,164	0.014	3.83
chr7:61,060,787-61,528,861	0.002	4.52
chr9:32,948,904-47,107,320	<0.001	6.16
chr9:65,212,784-69,851,859	<0.001	5.99
chr10:48,347,738-72,287,571	0.042	3.17
chr11:47,450,289-49,992,223	0.039	3.24
chr14:18,138,113-19,491,542	<0.001	5.15
chr15:18,317,177-20,332,186	0.050	3.05
chr17:41,809,072-42,128,170	0.039	3.27
chr20:27,100,000-28,191,516	0.012	3.90
chr21:9,882,805-10,202,296	<0.001	7.70

C

Frequent copy number gains associated with BRAF^{V600E} mutation

Genomic Region	Q-Bound	G-Score
chr1:199,122,306-200,611,035	0.003	4.02
chr6:37,258,122-41,526,454	<0.001	4.89
chr7:7,008,142-37,090,545	0.021	3.30
chr7:130,918,027-137,387,682	<0.001	4.63
chr8:140,373,779-146,274,826	<0.001	4.78
chr11:63,573,592-77,006,422	0.002	4.20
chr15:67,373,107-73,187,267	0.003	3.95
chr20:35,268,872-62,435,964	0.000	4.68
chr22:17,688,435-49,691,432	0.017	3.39

D

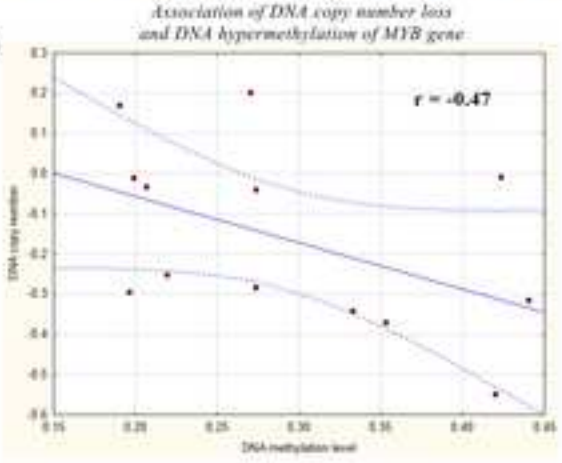

E

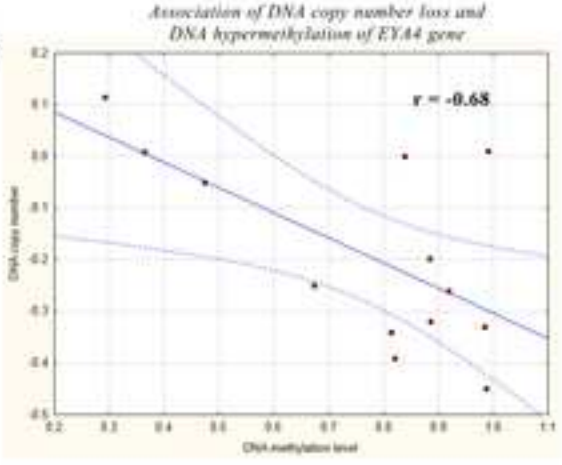

Figure_7
Click here to download high resolution image

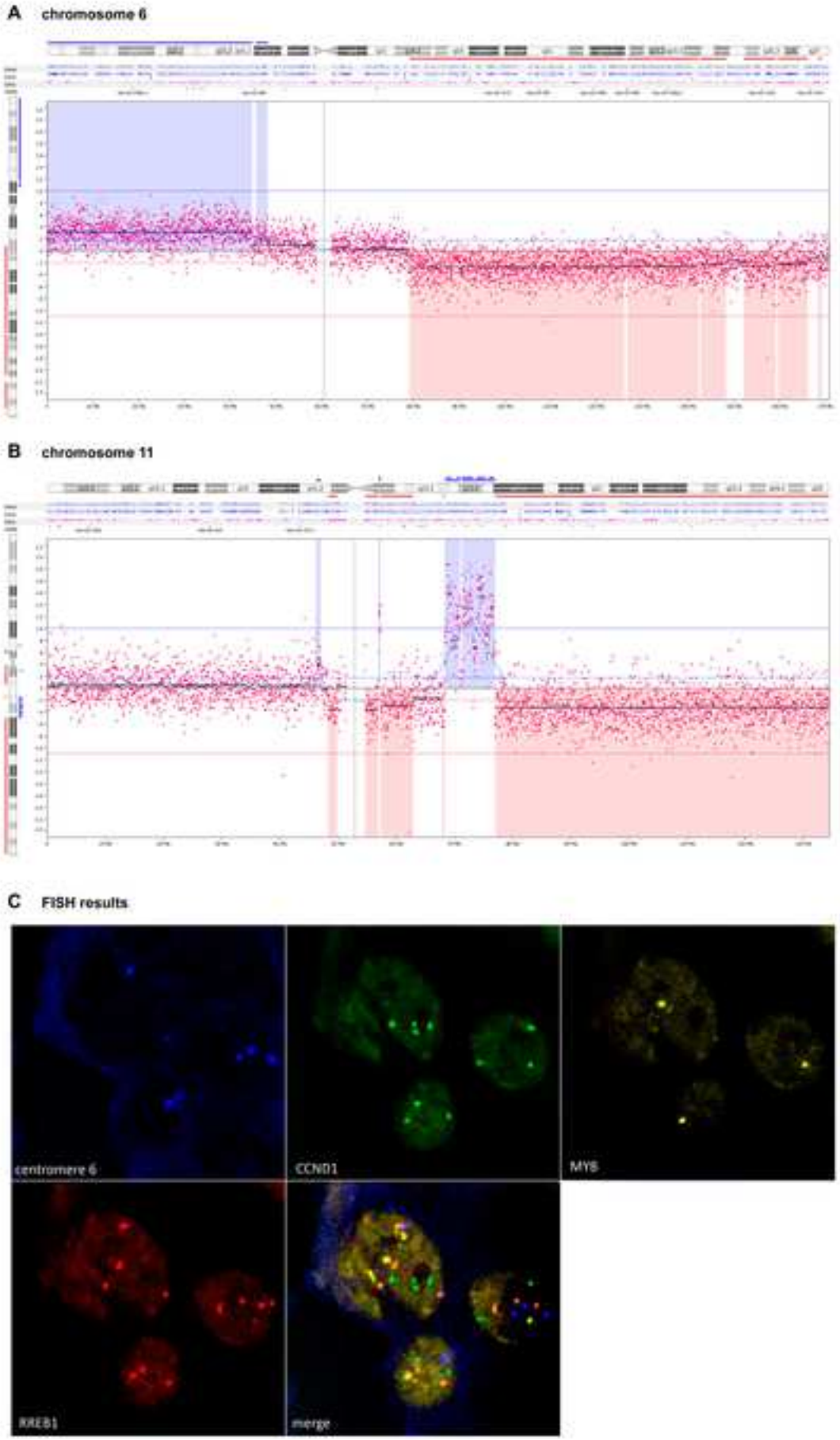

Supporting Information

Click here to download Supporting Information: Supplementary_Table_1_REVISED.xlsx

Supporting Information

Click here to download Supporting Information: Supplementary_Table_2.xlsx

Supporting Information

Click here to download Supporting Information: Supplementary_Table_3.xlsx

Supporting Information

Click here to download Supporting Information: Supplementary_Figure_1_new.pdf

~~DNA methylation is more characteristic of melanoma initiation than progression~~ DNA methylation characteristics of primary melanomas with distinct biological behaviour

Szilvia Ecsedi[1, 2], Hector Hernandez-Vargas[3], Sheila C. Lima[3], Laura Vizkeleti[1, 2], Reka Toth[1], Viktoria Lazar[1],Viktoria Koroknai[1], Timea Kiss[1], Gabriella Emri[4], Zdenko Herceg[3], Roza Adany[1,2] and Margit Balazs[1, 2]

[1]Department of Preventive Medicine, Faculty of Public Health, ~~Medical and Health Science Centre,~~ University of Debrecen, Hungary

[2]MTA-DE- Public Health Research Group ~~Public Health Research Group of the Hungarian Academy of Sciences,~~ University of Debrecen, Hungary

[3]International Agency for Research on Cancer, Section of Mechanisms of Carcinogenesis, Epigenetics Group, Lyon, France

[4]Department of Dermatology, Faculty of Medicine, ~~Medical and Health Science Centre,~~ University of Debrecen, Hungary

Corresponding author: Margit Balazs, Department of Preventive Medicine, Faculty of Public Health, University of Debrecen,

Debrecen 4028 Kassai út 26/b, Hungary; E-mail: balazs.margit@sph.unideb.hu

Keywords: primary melanoma, tumour progression, epigenetics, DNA methylation, hypermethylation, hypomethylation, copy number alteration, array CGH, BRAF mutation

Abstract

In melanoma, the presence of promoter related hypermethylation has previously been reported, however, no methylation-based distinction has been drawn among the diverse melanoma subtypes. Here, we investigated DNA methylation changes associated with melanoma progression and links between methylation patterns and other types of somatic alterations, including the most frequent mutations and DNA copy number changes.

Our results revealed that the methylome, presenting in early stage samples and associated with the $BRAF^{V600E}$ mutation, gradually decreased in the medium and late stages of the disease. An inverse relationship among the other predefined groups and promoter methylation was also revealed except for histologic subtype, whereas the more aggressive, nodular subtype melanomas exhibited hypermethylation as well. The Breslow thickness, which is a continuous variable, allowed for the most precise insight into how promoter methylation decreases from stage to stage. Integrating our methylation results with a high-throughput copy number alteration dataset, local correlations were detected in the MYB and EYA4 genes. With regard to the effects of DNA hypermethylation on melanoma patients' survival, correcting for clinical cofounders, only the KIT gene was associated with a lower overall survival rate.

In this study, we demonstrate the strong influence of promoter localized DNA methylation changes on melanoma initiation and show how hypermethylation decreases in melanomas associated with less favourable clinical outcomes. Furthermore, we establish the methylation pattern as part of an integrated apparatus of somatic DNA alterations.

Introduction

DNA methylation, along with covalent histone posttranslational modifications, chromatin remodelling and non-coding RNA-mediated gene interference, represents an important mechanism in the integrated apparatus of epigenetic regulation [1,2]. In addition to playing a role in several physiological processes [3,4,5], epigenetic mechanisms have been described as key factors in modifying the accessibility of DNA to transcription factors and, therefore, in altering the gene expression patterns of several cancer types [6,7,8]. Given the existence of relatively simple approaches that require even minute amounts of tumour DNA, the best factor described involved in melanoma epigenetics is DNA methylation, a covalent modification of mainly cytosines. The DNA hypermethylation is usually strictly localised to the transcriptionally active gene regions and promoters and directly inhibits gene expression. In the field of malignant melanoma epigenetics, there are substantial amounts of data available regarding gene silencing associated with the localised CpG hypermethylation of specific gene promoters. However, most of the provided data are derived from cell lines or were generated using single-gene approaches [9,10,11,12,13,14]. Despite the fact that some groups have attempted to conduct array-based experiments, to date, there are no methylation markers of the diverse melanoma subgroups based on a stratified analysis with sufficient statistical power [1]. Therefore, having chosen a powerful and high-throughput bead array technology, we performed array-based experiments to define the methylation pattern of 1,505 gene promoters. Previous studies have provided irrefutable proof of the reproducibility of this approach [6,7,15,16]. The simultaneous detection of transposonal demethylation and promoter methylation changes should provide valuable information regarding the molecular mechanisms potentially responsible for the aggressive phenotype of malignant melanoma. Recently, it has become widely accepted that Knudson's two-hit hypothesis is often confirmed through a combination of differing types of genomic alterations [17,18], which

prompted us to investigate whether methylation patterns are associated with other types of somatic alterations, such as the most frequent mutations (BRAF and NRAS) and DNA copy number (CN) alterations. Notable previous investigations demonstrated the prognostic relevance of CN aberrations [19,20,21,22]. Therefore, we also highlighted the cis-and trans-acting CN alterations of gene expression in malignant melanoma [23]. Moreover, we and others have demonstrated the association of BRAF and NRAS mutations with CN alterations using BAC arrays, suggesting a central role of BRAF mutations in gene copy number changes [21,24,25]. Additionally, a single group reported that the impact of BRAF signalling on gene methylation is widespread [26]. Despite the promising initial results, to our knowledge, no direct, array-based experiments have been performed in an integrative approach in a wide variety of primary melanomas. Therefore, we aimed to obtain better insight into how the DNA methylation changes are associated with distinct somatic alterations and contribute to melanoma progression.

Materials and Methods

Melanoma samples

Forty-two primary melanomas were included in Illumina bead assays. The clinicopathological data of the primary melanomas are summarised in Table 1.

The tumour tissues were obtained from the Department of Dermatology, University of Debrecen, Hungary. All human studies were conducted in accordance with the principles outlined in the Declaration of Helsinki, were approved by the Regional and Institutional Ethics Committee of the University of Debrecen Medical and Health Science Centre and were conducted according to regulations (Protocol #2836-2008). Written informed consent was obtained from each patient. The tumour diagnoses were made based on formalin-fixed

paraffin-embedded tissue sections using haematoxylin and eosin staining. The melanoma tumour staging was determined according to the new melanoma TNM staging system [27].

Genomic DNA and total RNA extraction

After surgical excision, the fresh tissues were immediately placed in RNA later solution (Applied Biosystems, Foster City, USA), and high-quality total RNA was prepared from the primary melanoma tissues using the RNeasy Mini Kit according to the supplier's protocol (Qiagen, GmbH, Germany). The obtained RNA concentrations were measured using a NanoDrop ND-1000 UV-Vis Spectrophotometer (Wilmington, Delaware, USA). The RNA sample integrity was determined with the Agilent 2100 Bioanalyser using the RNA 6000 Nano Kit (Agilent Technologies, Palo Alto, CA, USA). All RNA samples exhibited a 28S/18S ribosomal RNA ratio greater than 1.5.

The G-spin™ Genomic DNA Extraction Kit (Intron, Korea) was used to isolate high-molecular-weight DNA from primary melanomas according to the manufacturer's protocol. To determine the quantity of DNA obtained, we used a NanoDrop ND-1000 UV-Vis Spectrophotometer. The DNA integrity was verified via 1.2% agarose gel electrophoresis.

Bead Assay experiments

The quantitative methylation status of the 1505 CpG sites corresponding to 807 cancer-related gene promoters was determined using the Illumina GoldenGate Methylation Assay (Illumina, San Diego, CA, USA) on bisulphite-treated DNA samples corresponding to 42 primary melanomas. Bisulphite treatment was performed on 500 ng DNA using the EZ DNA Methylation-Gold Kit (Zymo Research). Duplicate samples were included to measure inter-array reproducibility for quality control. The GoldenGate assay consists of two allele-specific oligos (ASO) and two locus-specific oligos (LSO) for each CpG site. Each ASO–LSO oligo

Formatted: Font: Not Italic

pair corresponds to either the methylated or unmethylated state of the CpG site. Each methylation CpG spot is represented by two-color fluorescent signals from the M (methylated) and U (unmethylated) alleles. BeadStudio version 3.2 (Illumina) was used for obtaining the signal values (Avg-Beta) corresponding to the ratio of the fluorescent signal from the methylated allele (Cy5) to the sum of the fluorescents signals of both methylated (Cy5) and unmethylated alleles (Cy3), 0 corresponding to completely unmethylated sites and 1 to completely methylated sites. In agreement with the literature, 83 probes corresponding to the sex chromosomes were excluded to avoid any sex-specific bias. The probes with detection P values exceeding 0.01 in more than 10% of the specimens were removed from the analyses to exclude non-biological differences. As Du et al. performed a systematic comparison between Avg-Beta values and M-values, which is the logit transformation of Avg-Beta, and M-values were proven to be statistically valid for conducting differential methylation analysis [28]. M-values were used for class comparisons, whereas the raw Avg-Beta values were applied for correlation analyses (see at "Statistical Analysis").

Formatted: Font: Not Italic

~~The quantitative methylation status of the 1505 CpG sites corresponding to 807 cancer related gene promoters was determined using the Illumina GoldenGate Methylation Assay (Illumina, San Diego, CA, USA) on bisulphite treated DNA samples corresponding to 42 primary melanomas. Bisulphite treatment was performed on 500 ng DNA using the EZ DNA Methylation Gold Kit (Zymo Research). Duplicate samples were included to measure inter-array reproducibility for quality control. BeadStudio v3.2 Software (Illumina, San Diego, CA, USA) was used to obtain the signal values (Avg-Beta values). In agreement with the literature, 83 probes corresponding to the sex chromosomes were excluded to avoid any sex-specific bias [8]. The probes with detection P values exceeding 0.01 in more than 10% of the specimens were removed from the analyses to exclude non-biological differences. Therefore, 895 CpG probes remained for further analyses.~~

Array CGH for studying copy number alterations

The results data of our previous Tiling Array CGH (HG18 CGH 4x72K WG Tiling v2.0) experiments (Roche NimbleGen core facility, Reykjavik, Iceland) were used which can be found under the following accession number: E-MTAB-947 (Array Express Archive repository).

The GISTIC algorithm was used to identify regions containing a statistically high frequency of copy number aberrations compared to the "background" aberration frequency. This function is most appropriate for cancer samples, as it was designed using a cancer dataset [29]. After the gain/loss aberrations were identified in each sample, a statistic (the G score) was calculated for each aberration. This G score is a measure of the frequency of occurrence of the aberration and the magnitude of the copy number change (log ratio intensity) at each location in the aggregate of all samples in the dataset. Each location is scored separately for gains and losses. The locations in each sample are permuted, simulating data with random aberrations, and this random distribution is compared to the observed statistic to identify scores that are unlikely to occur by chance alone.

Array CGH results were verified using four colour FISH (Abott Molecular Inc., USA). The FISH experiments were performed according to the Suppliers' protocol and visualized by Zeiss Axio Imager Confocal Microscopy.

Quantitative RT-PCR

The expression status of selected genes (FGFR3, MCAM and IL8) was measured using quantitative real-time PCR with the ABI Prism® 7900HT Sequence Detection System (Applied Biosystems, Carlsbad, California, USA). Reverse transcription (RT) was carried out on total RNA (600 ng) using the High Capacity cDNA Archive Kit, according to the protocol of the supplier (Applied Biosystems, Carlsbad, California, USA). Predesigned TaqMan® Gene Expression Assays (Applied Biosystems, Carlsbad, California, USA) were used to perform qPCR for the abovementioned 3 genes.

Statistical analyses

The effect of localised methylation on clinical predictors, BRAF^{V600E} mutation and patient survival

To compare the methylation patterns between primary melanoma groups detailed in Table 1, we applied random variance t-statistics on all the binary data classes such as Breslow thickness with the cut-off value of 4 mm; metastasis, ulceration and histologic subtype. Being continuous variable, Breslow thickness can be divided into more subgroups: according to the TNM system up to 5 groups can be created, however, due to the limitation of smaller samples, developing 3 groups based on the cut-off values of 2mm and 4mm were the most ideal. F-statistics was applied on the trichotomised Breslow groups for each CpG site.

CpG sites were considered differentially methylated when their p values based on univariate t-tests or f-tests were less than 0.01; in addition, given CpG sites were identified differentially methylated between the melanoma subgroups based on a multivariate permutation test providing 90% confidence that the false discovery rate was less than 20%. Volcano plots were applied to illustrate differential methylation patterns among clinical subgroups of melanomas (the clinicopathological characteristics of melanomas are summarized in Table 1). Volcano

plots combine p-values of the t-tests for each CpG sites and ratios between the melanoma subgroups. Additionally, the trichotomised Breslow thickness groups were visualized by heatmap and compared by Principal Component Analysis (PCA).

For the aforementioned class comparisons, M-values, the logit transformations of signal intensities were used.

~~We attempted to estimate whether the specifically methylated gene pattern exists in primary melanomas. For this purpose, we applied the following criteria: CpG sites were considered differentially methylated when their p values were less than 0.01; in addition, given CpG sites were identified differentially methylated between the melanoma subgroups based on a multivariate permutation test providing 90% confidence that the false discovery rate was less than 20%.~~

To evaluate the KEGG-based gene networks disturbed by DNA methylation, we applied the Efron-Tibshirani Gene Set Analysis that uses 'maxmean' statistics to identify gene sets expressed differentially among predefined classes [30]. The threshold for determining significant gene sets was 0.01 in each approach.

The Cox proportional univariate approach was performed on each gene to test whether the methylation status of a particular gene significantly influences the survival at the $p < 0.05$ level. To control for covariates on survival and to predict the survival risk, the Supervised Principal Components method was used.

As normal tissues were not involved in or studies we used external dataset from the study of Conway et al. involved 27 naevi [15] to check the methylation status of a given gene in control tissues.

Remaining statistics were performed using SPSS 19.0 and GraphPad Prism 6.0 demo version. Venn diagram was made by VENNY, an interactive tool for comparing lists with Venn

Diagrams developed by Oliveros, J.C. (2007). The tool is available at: http://bioinfogp.cnb.csic.es/tools/venny/index.html.

Relationship between methylation patterns and copy number alterations

We studied how DNA copy number changes and methylation pattern associated within the same genetic loci. For this purpose, the copy number and localised methylation data of the corresponding genomic regions were simultaneously analysed gene-by-gene using CGH Tools, and Pearson's correlation was performed with $p<0.01$ after correction for multiple testing. Additionally, Fisher's exact test was applied to identify the genome sequences where gene methylation occurs frequently.

Results

Methylation patterns of melanoma subgroups

Our experimental design for applying the Illumina Bead Assay included two replicate samples among arrays to measure the inter-array reproducibility. Technical replicates were significantly correlated with each other by Pearson's correlation (Replicate #1: $r^2= 0.95$, $p<0.001$; Replicate #2: $r^2= 0.98$, $p< 0.001$).

After the initial filtering process, 895 CpG sites were available for further analyses and M-values, logistically transformed Avg-Beta values, were used for statistical approaches.

Our main goal was to investigate the relationship between the distinct biological types of melanomas and the promoter methylation levels. As the multivariate permutation test provides a tight probabilistic control on the proportion of false discoveries, this test was used for class comparison on each predefined subgroup (the clinical subgroups of primary melanomas are detailed in Table 1) according to the following criteria: CpG sites were

considered differentially methylated when their p values were less than 0.01 and FDR rates were below 0.2.

Figure 1A demonstrates that relatively large number of CpG sites was found to be differentially methylated between melanoma subgroups. Interestingly, the majority of these CpGs were characterised by decreased DNA methylation levels in samples with poor prognosis (larger than 4 mm, metastatic, ulcerated and nodular primary melanomas). Histologic subtype exhibited a more disturbed methylation pattern involving high number of differentially methylated genes in both superficial and nodular subtype. As it can be seen in Figure 1A, some of the differentially methylated individual genes were represented by more than one significant CpG sites arguing in favour of the consistency of given alterations. Altogether, 111 differentially methylated genes were identified in the context of aforementioned clinical predictors: 43 individual genes were hypermethylated and 68 genes hypomethylated in melanomas with less favourable clinical outcome. The differentially methylated gene lists specific for the Breslow thickness, ulceration, metastatic capacity and histologic subtype are detailed in Supplementary Table 1. Venn diagrams (Figure 1B) indicate the common properties among genes with decreased and increased DNA methylation, respectively.

~~Figure 1A demonstrates that relatively large number of CpG sites was found to be differentially methylated between melanoma subgroups. The majority of these CpGs were hypermethylated in smaller (less than 4 mm) and non-ulcerated melanomas as well as specimens without metastatic capacity. Histologic subtype exhibited a more disturbed methylation pattern involving high number of hypermethylated genes in both superficial and nodular subtype. As it can be seen in Figure 1A, some of the differentially methylated individual genes were represented by more than one significant CpG sites arguing in favour of the consistency of given alterations. Altogether, 111 differentially methylated genes were~~

~~identified in the context of aforementioned clinical predictors. The differentially methylated gene lists specific for the Breslow thickness, ulceration, metastatic capacity and histologic subtype are detailed in Supplementary Table 1. A Venn diagram (Figure 1B) indicates the common properties among methylated elements of clinical parameters, e.g., Breslow thickness, ulceration, metastasis formation and histological subtype.~~

Being a continuous variable, Breslow thickness allowed the most precise insight into how methylation pattern changes across melanoma stages. In Figure 2A, the heatmap horizontally shows the primary melanoma samples with distinct Breslow thicknesses. The intensive hypermethylation of 45 CpGs is marked with brown colour in the early stage tumours (Breslow thickness < 2mm), and this hypermethylation decreases during the medium and advanced stages. Low-level methylation values are represented with yellow colour. In other types of cancer, hypermethylation has been shown to be associated with tumour progression. Interestingly, the hypermethylation patterns of 45 CpGs, which are detected in the early stages of melanomas, gradually decrease in the medium stages and almost disappear in late stages of the disease. The Principal Component Analysis (Figure 2B) clearly demonstrated that, according to the pattern of the 45 hypermethylated CpGs, the melanoma groups were significantly separated.

It is important to note that normal tissues were not used in our experiments. However, such datasets can be found in the literature, and we were therefore able to correct for the methylation status of normal naevi specimens (see Materials and Methods). These results thus argue that the hypermethylation of the 45 CpGs occurs early, in melanomas less than 2 mm, and then decreases during melanoma progression.

In addition to individual gene signatures, we aimed to determine whether the perturbed KEGG-based gene networks are related to localised methylation patterns. We did not identify any perturbed pathways among clinical subgroups, however, as shown in Figure 3A-B, Cell

communication and ECM-receptor interaction networks were found to be significant at the 0.01 level between $BRAF^{V600E}$ mutant and wild type samples. (The full list of CpG probes is given in Supplementary Table 2). Interestingly, there was poor overlap (Figure 3C) between differentially methylated genes associated with $BRAF^{V600E}$ mutation and clinical subgroups discussed above.

Our analysis of the effects of hypermethylation on patient survival identified an association between six hypermethylated genes (DSP, EPHB6, HCK, IL18, IRAK3 and KIT) with lower OS values. Four of the six genes (DSP, HCK, IL18 and KIT) exhibited significantly different Kaplan-Meier curves (Figure 4). However, when we included patient age, gender and $BRAF^{V600E}$ mutation status in the survival risk prediction model, only the KIT gene remained significant.

Analysis of the mRNA expression level of the differentially methylated genes identified in melanoma

Three genes among the differentially methylated panel were chosen to measure mRNA expression levels by qPCR (FGFR3, MCAM and IL8) according to the following selection criteria: we exclusively focused on genes that had not been previously referred to as methylated in melanomas; furthermore, FGFR3 was chosen in the context of histologic subtype and MCAM of Breslow thickness, while IL8, being a commonly methylated gene among distinct clinical groups was measured across in all categories (Breslow thickness, histologic subtype, ulceration and metastatic capacity).

Inverse relationships were found between hypermethylation and mRNA expression regarding FGFR3, MCAM and IL8 as well, supporting the notion that the methylation pattern are functionally relevant to gene expression. Significant ($p<0.05$) MCAM mRNA expression level differences were revealed between smaller (Breslow thickness $\leq$ 4mm) and larger

(Breslow thickness > 4mm) melanomas. IL8 expression differed as well between sample distinct categories of Breslow thickness, melanoma surface ulceration and metastatic capacity. The qPCR and corresponding correlation results are summarised in Figure 5.

Coincidence of localised hypermethylation and copy number alterations

We determined the frequent copy number gains and losses associated with the $BRAF^{V600E}$ mutation (Figure 6A) and Breslow thickness (Supplementary Table 3) in primary melanomas. As expected, a set of marked copy number alterations was associated with both the $BRAF^{V600E}$ (Figure 6A) mutation and Breslow thickness (Supplementary Table 3) categories.

In the $BRAF^{V600E}$ mutant samples, significant CN losses (Figure 6B) were found at in the 1p, 1q, 2p, 4q, 6q, 7p, 9p, 9q, 10p, 10q, 11p, 14p, 15p, 17p, 20p and 21p regions, whereas CN gains (Figure 6C) were detected across chromosomes 1q, 6p, 7p, 7q, 8q, 11q, 15q, 20q and 22q.

In the late stages of primary melanomas (Breslow thickness > 4mm), significant CN losses were observed more frequently and comprised deletions of 1p, 4q, 7p, 9p, 14p and 21p, whereas CN gains were only observed in the 11q region, as summarised in Supplementary Table 3. Despite not reaching a significant level, it is worth noting that the CN losses in 19p12 (harbouring the DNA Methyltransferase-1 gene) were exclusively associated with more advanced stages (Breslow thickness > 2mm; Supplementary Figure 1A). However, among the late-stage samples (Breslow thickness > 4mm), CN gains were also found with CN losses in some samples. Supplementary Figure 1B-D represents late-stage melanomas that exhibited CN losses in 19p12.

In addition to the general mapping of the CN-altered genomic regions, we quantitatively assessed the coincidence of CN alteration and methylation patterns gene by gene. Similar to other studies, we established gene level measurements by averaging the methylation states

within gene-specific regions. As significantly and positively correlated genes were revealed at the levels of methylation and CN alteration, the correlations cannot possibly represent coordinated allele loss and hypermethylation; nevertheless, these results do not remain significant after the multiple correction procedure. Moreover, direct correlation often involves genome parts that are positively correlated at the level of methylation and CN without detected CN changes or altered methylation. Therefore, we applied an alternative approach based on the frequency of methylated genes harbouring significant CN alterations to test Knudson's two-hit hypothesis. As indicated in Figure 6A, 6q12-6q25.1 comprises a relatively large, significant CN loss and two hypermethylated genes, namely, EYA4 (6q23) and MYB (6q22-q23). When measured quantitatively, a significant inverse correlation was observed between CN loss and DNA hypermethylation (Figure 6 D-E).

Array CGH results were further confirmed by four colour FISH experiments specific for 11q13 (specific for CCND1 gene), 6p25 (specific for RREB1 gene), 6q23 (specific for MYB gene) and centromere 6 on 27 primary melanomas (Figure 7A-C).

Discussion

Among epigenetic aberrations, DNA methylation itself features a diverse presence [31]. Recently, 5-hydroxymethylcytosine (5-hmC) has been identified as a constituent of mammalian DNA and described as the sixth base of the genome [32]. The loss of 5-hmC has been highlighted as a hallmark of melanoma by a single, remarkable study, whereas interesting clues as to the role of 5-hydroxymethylcytosine are still emerging [33]. In contrast to 5-hmC, the importance of 5-methylcytosine (5-mC) in cancer cells is much more firmly established [1,34]. Aberrant promoter DNA hypermethylation or localised methylation preferably occurs in CpG dinucleotide-dense regions, resulting in the down-regulation of the corresponding gene [1,14].

It has recently become apparent that malignant melanomas feature hypermethylation, and currently more than 80 genes – mainly in promoter regions – are hypermethylated at a single-gene level [1,12,31]. Taking a global view of the available data, the number of primary tumour samples involved in the studies and the frequency of positive results do not allow determining whether the hypermethylated genes described are appropriate for diagnosis or can be considered candidate therapeutic targets. Moreover, most of the data provided are derived from cell lines and estimated methylation values indirectly consisting of three steps: measuring mRNA or protein expression in cell lines, treating samples with a specific drug that acts against the process of methylation and measuring gene expression again. Nonetheless, powerful arguments have been presented in the literature that support direct experiments being less ambiguous; furthermore, most of the groups conducting direct measurements have applied candidate gene approaches [31,35].

In addition to the rapid progress that has been made in studying promoter hypermethylation at the single-gene level, only two groups have attempted to conduct array-based experiments to identify the methylation pattern of thousands of gene promoters [15,36]. Regrettably, one group has focused only on comparing the methylation level of primary invasive melanomas with benign melanocytes and has clearly identified a group of genes in a statistically powerful interpretation that can be used to discriminate naevi from melanomas based on their methylation signature [15]. Another group has examined the short-term cultures of homogeneous stage III specimens [36].

As no data are currently available regarding the methylation markers of diverse melanomas with different clinical behaviours, we performed a systematic comparison of localised methylation patterns among 42 primary melanomas using the Illumina Golden Gate Cancer Panel Bead Assay. We found 111 differentially methylated CpGs altogether among melanoma subgroups and the majority of CpG sites were hypermethylated in melanomas that represent

more favourable prognoses including a non-ulcerated tumour surface, superficial spreading histological subtype, non-metastatic subgroup and smaller tumour thickness (Breslow thickness < 2 mm). Regarding more advanced-stage specimens, the hypermethylome detected in melanomas that represents better prognoses markedly decreased. The decrease in the methylation levels occurred gradually, as the continuous Breslow thickness variables allowed us to distinguish more than two groups among primary melanomas and to map the progress of demethylation during distinct stages (Breslow thickness < 2 mm; Breslow thickness 2 - 4 mm; Breslow thickness > 4 mm). The genes involved in demethylation partially overlap among clinical subgroups: five ~~six~~ genes (EMR3, SEPT9, IL8, MMP14~~, MMP19~~ and SLC22A18) were found to be commonly demethylated in large (Breslow thickness > 4 mm), nodular subtype, ulcerated and metastatic melanomas. The SEPT9 gene is an ovarian tumour suppressor playing a role in cell cycle control [37]; IL8 gene expression is elevated in metastatic melanomas and can increase the level of MMP2 [38]; SLC22A18 has been reported to be down-regulated due to promoter hypermethylation in gliomas [38,39]; MMP14 has not been found to play a role in melanoma progression thus far. Among the aforementioned clinical groups, the largest similarity (27 overlapping genes) has been detected between the demethylated genes associated with Breslow thickness and ulceration. The histologic subtype represents the most unique methylation pattern, comprising 30 differentially methylated genes between superficial and nodular melanomas.

Our results contrast those of studies describing the hypermethylation patterns of specific genes as tumour progression-related markers based on single gene approaches. However, Conway et al. supported the claim that a covalent change from cytosine to 5-methylcytosine in the promoter region occurs as an early aberration event in melanomas [15]. Notwithstanding, their results highlighted not only the hypermethylated but also the demethylated genes in heterogeneous melanomas compared to naevi. This group reported a

lack of similarity – involving only two genes, namely, RUNX3 and SYK – with the previously published data.

Previously, a group published two independent studies regarding in vitro data that demonstrated how the BRAF^{V600E} mutation causes widespread alterations in DNA methylation [26,40]. ~~Along with Hou et al., we found hypermethylated CpGs accompanied by the BRAF^{V600E} mutation in primary melanomas.~~ In agreement with these observations, we also found distinct methylation pattern in BRAF^{V600E} mutant primary melanomas involving genes of Cell Communication and ECM-receptor interaction networks. A similar association between the BRAF^{V600E} mutation and DNA methylation was described in colon cancer, as methylated samples convincingly represented a distinct subset encompassing almost all cases of tumours with the BRAF^{V600E} mutation [41]. A remarkable study performed by Roon et al. revealed the *BRAF^{V600E}* mutation-specific hypermethylation of CpG regions in colon cancer samples by Differential Methylation Hybridization on high-density oligonucleotide microarrays. Interestingly, the authors identified several cancer-related pathways, including the PI3 kinase and Wnt signaling pathways being differentially methylated between BRAF^{V600E} mutant and wild type samples. Additionally, the group found the silencing of *FOXD3 hypermethylated manner*. Based on these studies, authors suggest that a specific epigenetic pattern can contribute to a favorable context for the acquisition of *BRAF^{V600E}* mutations. However, further studies are warranted to further clarify the relationship between the mutation and DNA methylation.

In addition to the common mutations, specific patterns of CN alterations have been reported in melanomas characteristic of unfavourable clinical outcomes [21]. Furthermore, it has become obvious that BRAF^{V600E} mutated melanomas display distinct patterns for CN changes, providing the first line of evidence in support of Knudson's two-hit hypothesis [19,21]. However, none of the published studies attempted to evaluate the relationship

between CN alterations and DNA methylation in melanomas. Our group performed a Tiling Array CGH, and, apart from highlighting common CN losses and amplification in the subgroups of primary melanomas, we demonstrated that 6q12-6q25.1 comprises a remarkable CN loss, harbouring two hypermethylated genes on 6q23, EYA4 and MYB1. This result was measured and verified quantitatively and provides evidence for Knudson's two-hit hypothesis at the level of CN loss and DNA hypermethylation. Notably, MYB1 is an important discriminator between melanomas and naevi, as validated by FISH in 123 melanomas and 110 naevi [42,43]. The copy number deletion of MYB1 is currently used in the diagnosis of melanoma.

Our Tiling Array CGH experiments showed another important feature: the CN alterations of chromosome 19 were only detected in advanced staged primary melanomas. Notably, the altered genomic regions encompass 19p13.2, which harbours the DNMT1 gene (DNA Methyltransferase-1), which plays a role in the establishment and regulation of tissue-specific patterns of methylated cytosine residues [31]. The DNA CN alterations of DNMT1 in advanced stages primary melanomas raise crucial questions: Is demethylation, contributing to clinical outcomes, only a passive consequence of CN loss? Or do CN alterations – as was demonstrated in the context of epigenetic mechanisms and the $BRAF^{V600E}$ mutation – directly control the DNA methylation changes to influence the gene expression patterns of given molecules? Regardless of the reason for changes in methylation, we obtained better insight into how gene expression levels are regulated by DNA methylation: demethylation was associated with increased mRNA levels, whereas hypermethylation was associated with decreased levels.

In summary, we demonstrated the strong influence of DNA methylation changes on melanoma progression. However, hypermethylation, which has been greatly emphasised in the literature, appears to represent more complexity both in melanoma initiation and

progression. Additionally, the inhibition of promoter hypermethylation might represent the most promising therapeutic target for the treatment of melanoma, and several types of DNMT inhibitors are currently being developed [35]. Considering the dual role of DNA methylation, further efforts are needed to investigate the importance of such drugs in melanoma treatment.

Acknowledgments

DNA methylation date analyses were performed using BRB-ArrayTools developed by Dr. Richard Simon and BRB-Array Tools Development Team. We thank Orsolya Papp for the assistance of microscopic analysis of the FISH experiments.

References

1. van den Hurk K, Niessen HE, Veeck J, van den Oord JJ, van Steensel MA, et al. (2012) Genetics and epigenetics of cutaneous malignant melanoma: a concert out of tune. Biochim Biophys Acta 1826: 89-102.
2. Heyn H, Esteller M (2012) DNA methylation profiling in the clinic: applications and challenges. Nat Rev Genet 13: 679-692.
3. Wild L, Flanagan JM (2010) Genome-wide hypomethylation in cancer may be a passive consequence of transformation. Biochim Biophys Acta 1806: 50-57.
4. James SJ, Pogribny IP, Pogribna M, Miller BJ, Jernigan S, et al. (2003) Mechanisms of DNA damage, DNA hypomethylation, and tumor progression in the folate/methyl-deficient rat model of hepatocarcinogenesis. J Nutr 133: 3740S-3747S.
5. Acquaviva L, Szekvolgyi L, Dichtl B, Dichtl BS, de La Roche Saint Andre C, et al. (2013) The COMPASS subunit Spp1 links histone methylation to initiation of meiotic recombination. Science 339: 215-218.
6. Hernandez-Vargas H, Ouzounova M, Le Calvez-Kelm F, Lambert MP, McKay-Chopin S, et al. (2011) Methylome analysis reveals Jak-STAT pathway deregulation in putative breast cancer stem cells. Epigenetics 6: 428-439.
7. Lima SC, Hernandez-Vargas H, Simao T, Durand G, Kruel CD, et al. (2011) Identification of a DNA methylome signature of esophageal squamous cell carcinoma and potential epigenetic biomarkers. Epigenetics 6: 1217-1227.
8. Hernandez-Vargas H, Lambert MP, Le Calvez-Kelm F, Gouysse G, McKay-Chopin S, et al. (2010) Hepatocellular carcinoma displays distinct DNA methylation signatures with potential as clinical predictors. PLoS One 5: e9749.
9. Furuta J, Umebayashi Y, Miyamoto K, Kikuchi K, Otsuka F, et al. (2004) Promoter methylation profiling of 30 genes in human malignant melanoma. Cancer Sci 95: 962-968.
10. Marini A, Mirmohammadsadegh A, Nambiar S, Gustrau A, Ruzicka T, et al. (2006) Epigenetic inactivation of tumor suppressor genes in serum of patients with cutaneous melanoma. J Invest Dermatol 126: 422-431.
11. Mori T, Martinez SR, O'Day SJ, Morton DL, Umetani N, et al. (2006) Estrogen receptor-alpha methylation predicts melanoma progression. Cancer Res 66: 6692-6698.
12. Liu S, Ren S, Howell P, Fodstad O, Riker AI (2008) Identification of novel epigenetically modified genes in human melanoma via promoter methylation gene profiling. Pigment Cell Melanoma Res 21: 545-558.
13. Lahtz C, Stranzenbach R, Fiedler E, Helmbold P, Dammann RH (2010) Methylation of PTEN as a prognostic factor in malignant melanoma of the skin. J Invest Dermatol 130: 620-622.
14. Sigalotti L, Covre A, Fratta E, Parisi G, Colizzi F, et al. (2010) Epigenetics of human cutaneous melanoma: setting the stage for new therapeutic strategies. J Transl Med 8: 56.
15. Conway K, Edmiston SN, Khondker ZS, Groben PA, Zhou X, et al. (2011) DNA-methylation profiling distinguishes malignant melanomas from benign nevi. Pigment Cell Melanoma Res 24: 352-360.
16. Bibikova M, Le J, Barnes B, Saedinia-Melnyk S, Zhou L, et al. (2009) Genome-wide DNA methylation profiling using Infinium(R) assay. Epigenomics 1: 177-200.
17. Houseman EA, Christensen BC, Karagas MR, Wrensch MR, Nelson HH, et al. (2009) Copy number variation has little impact on bead-array-based measures of DNA methylation. Bioinformatics 25: 1999-2005.

18. Christensen BC, Houseman EA, Poage GM, Godleski JJ, Bueno R, et al. (2010) Integrated profiling reveals a global correlation between epigenetic and genetic alterations in mesothelioma. Cancer Res 70: 5686-5694.
19. Rose AE, Poliseno L, Wang J, Clark M, Pearlman A, et al. (2011) Integrative genomics identifies molecular alterations that challenge the linear model of melanoma progression. Cancer Res 71: 2561-2571.
20. Berger MF, Garraway LA (2009) Applications of genomics in melanoma oncogene discovery. Hematol Oncol Clin North Am 23: 397-414, vii.
21. Lazar V, Ecsedi S, Vizkeleti L, Rakosy Z, Boross G, et al. (2012) Marked genetic differences between BRAF and NRAS mutated primary melanomas as revealed by array comparative genomic hybridization. Melanoma Res 22: 202-214.
22. Vizkeleti L, Ecsedi S, Rakosy Z, Orosz A, Lazar V, et al. (2012) The role of CCND1 alterations during the progression of cutaneous malignant melanoma. Tumour Biol 33: 2189-2199.
23. Rakosy Z, Ecsedi S, Toth R, Vizkeleti L, Herandez-Vargas H, et al. (2013) Integrative genomics identifies gene signature associated with melanoma ulceration. PLoS One 8: e54958.
24. Thomas NE (2006) BRAF somatic mutations in malignant melanoma and melanocytic naevi. Melanoma Res 16: 97-103.
25. Greshock J, Nathanson K, Medina A, Ward MR, Herlyn M, et al. (2009) Distinct patterns of DNA copy number alterations associate with BRAF mutations in melanomas and melanoma-derived cell lines. Genes Chromosomes Cancer 48: 419-428.
26. Hou P, Liu D, Dong J, Xing M (2012) The BRAF(V600E) causes widespread alterations in gene methylation in the genome of melanoma cells. Cell Cycle 11: 286-295.
27. Gershenwald JE, Soong SJ, Balch CM (2010) 2010 TNM staging system for cutaneous melanoma...and beyond. Ann Surg Oncol 17: 1475-1477.
28. Du P, Zhang X, Huang CC, Jafari N, Kibbe WA, et al. (2010) Comparison of Beta-value and M-value methods for quantifying methylation levels by microarray analysis. BMC Bioinformatics 11: 587.
29. Beroukhim R, Getz G, Nghiemphu L, Barretina J, Hsueh T, et al. (2007) Assessing the significance of chromosomal aberrations in cancer: methodology and application to glioma. Proc Natl Acad Sci U S A 104: 20007-20012.
30. Tibshirani R, Hastie T, Narasimhan B, Chu G (2002) Diagnosis of multiple cancer types by shrunken centroids of gene expression. Proc Natl Acad Sci U S A 99: 6567-6572.
31. Balazs M, Ecsedi, S., Vizkeleti, L., Begany, A., (2011) Genomics of human malignant melanoma. In: Tanaka IY, editor. Breakthroughs in melanoma research. Rijeka: InTech. pp. pp. 237-263.
32. Song CX, He C (2011) The hunt for 5-hydroxymethylcytosine: the sixth base. Epigenomics 3: 521-523.
33. Lian CG, Xu Y, Ceol C, Wu F, Larson A, et al. (2012) Loss of 5-hydroxymethylcytosine is an epigenetic hallmark of melanoma. Cell 150: 1135-1146.
34. Tellez CS, Shen L, Estecio MR, Jelinek J, Gershenwald JE, et al. (2009) CpG island methylation profiling in human melanoma cell lines. Melanoma Res 19: 146-155.
35. Adjemian JZ, Howell J, Holzbauer S, Harris J, Recuenco S, et al. (2009) A clustering of immune-mediated polyradiculoneuropathy among swine abattoir workers exposed to aerosolized porcine brains, Indiana, United States. Int J Occup Environ Health 15: 331-338.
36. Sigalotti L, Covre A, Fratta E, Parisi G, Sonego P, et al. (2012) Whole genome methylation profiles as independent markers of survival in stage IIIC melanoma patients. J Transl Med 10: 185.

37. Scott M, McCluggage WG, Hillan KJ, Hall PA, Russell SE (2006) Altered patterns of transcription of the septin gene, SEPT9, in ovarian tumorigenesis. Int J Cancer 118: 1325-1329.
38. Zhang H, Fu T, McGettigan S, Kumar S, Liu S, et al. (2011) IL8 and Cathepsin B as Melanoma Serum Biomarkers. Int J Mol Sci 12: 1505-1518.
39. Chu SH, Feng DF, Ma YB, Zhang H, Zhu ZA, et al. (2011) Promoter methylation and downregulation of SLC22A18 are associated with the development and progression of human glioma. J Transl Med 9: 156.
40. Liu D, Liu X, Xing M (2012) Epigenetic genes regulated by the BRAFV600E signaling are associated with alterations in the methylation and expression of tumor suppressor genes and patient survival in melanoma. Biochem Biophys Res Commun 425: 45-50.
41. Bae JM, Kim JH, Kang GH (2013) Epigenetic alterations in colorectal cancer: the CpG island methylator phenotype. Histol Histopathol.
42. Senetta R, Paglierani M, Massi D (2012) Fluorescence in-situ hybridization analysis for melanoma diagnosis. Histopathology 60: 706-714.
43. Gerami P, Li G, Pouryazdanparast P, Blondin B, Beilfuss B, et al. (2012) A highly specific and discriminatory FISH assay for distinguishing between benign and malignant melanocytic neoplasms. Am J Surg Pathol 36: 808-817.

Figure legends

~~**Figure 1 Methylation patterns of primary melanomas associated with known clinical predictors**~~

~~**(A)** Volcano plots of differentially methylated genes associated with the known predictors (e.g. Breslow thickness, metastatic capacity, ulceration, histologic subtype) of primary melanomas. Relatively large numbers of genes were found to be hypermethylated in samples characteristic for favourable outcome compared to melanomas with poor prognosis. **(B)** A Venn diagram indicates the overlap of methylated genes among the four types of clinical predictors.~~

Figure 1 DNA Methylation patterns of primary melanomas with known clinical predictors

(A) Volcano plots of differentially methylated genes associated with known predictors. Blue dots indicates decreased and red indicates increased methylation as follows: Breslow thickness: 51 hypomethylated probes (43 individual genes) and 5 hypermethylated probes (5 individual genes); metastatic capacity: 23 hypomethylated probes (21 individual genes) and 5 hypermethylated probes (4 individual genes), ulceration: 48 hypomethylated probes (43 individual genes) and 8 hypomethylated probes (8 individual genes), histologic subtype: 28 hypomethylated probes (26 individual genes) 23 hypermethylated probes (20 individual genes) **(B)** A Venn diagrams indicate the overlap of differentially methylated genes (in left: number of hypomethylated genes; in right: number of hypermethylated genes) for each clinical predictor class.

Figure 2 Hypermethylation is an early event in melanomas and decreases with tumour thickness

(A) The heatmap demonstrates the hypermethylation patterns (indicated in brown colour) of 45 CpGs, which can be detected in the early stages of melanomas (horizontal purple colour) but decrease from the medium stage (horizontal green colour) to the late stage (horizontal blue colour). **(B)** The principal component analysis for the distinction of the Breslow thickness the sample groups (large: blue dots; medium: green dots; and small melanoma samples: purple dots) based on the 45 differentially methylated CpGs. The analysis revealed that, according to the first three components, which covered the 56% of the total variance, the three groups were significantly different ($p < 0.05$)

~~**Figure 3 Differentially methylated gene sets between the BRAF^{V600E} mutant and wild-type classes**~~

~~**(A)** Differentially methylated gene sets between the BRAF^{V600E} mutant and wild type classes according to the Kyoto Encyclopaedia of Genes and Genomes. **(B)** Average log-ratios of Avg Beta methylation values in BRAF^{V600E} mutant and wild type melanomas. Red indicates significant genes associated with ECM receptor interaction and blue depicts significant genes on Cell communication pathway. (Eleven genes overlap between the ECM receptor interaction and Cell communication.) **(C)** Venn diagram shows lack of overlap between differentially methylated genes associated with BRAF^{V600E} mutation and the known clinical predictors as Breslow thickness, metastatic capacity, ulceration and histologic subtype.~~

Figure 3 Differentially methylated gene sets between melanoma classes

(A) Differentially methylated gene sets between BRAF^{V600E} mutant and wild-type, metastatic and non-metastatic, ulcerated and non-ulcerated classes according to the Kyoto Encyclopaedia of Genes and Genomes. **(B)** Average log-ratios of methylation intensities in BRAF^{V600E} mutant and wild-type melanomas. Red indicates significant genes associated with ECM-receptor interaction and blue depicts significant genes on Cell communication pathway. (Eleven genes overlap between the ECM-receptor interaction and Cell communication.) **(C)** Venn diagram shows lack of overlap between differentially methylated genes associated with BRAF^{V600E} mutation and the known clinical predictors as Breslow thickness, metastatic capacity, ulceration and histologic subtype.

Formatted: Font: Not Italic

~~**Figure 4 Hypermethylated genes associated with decreased survival rate in melanoma patients**~~

~~The Kaplan-Meier curves for genes (DSP, EPHB6, HCK, IL18, IRAK3 and KIT) whose hypermethylation was associated with a lower overall survival rate; the Cox proportional univariate approach was performed on each gene to test whether a methylation status of a particular gene significantly influences the survival at the $p < 0.05$ level.~~

Figure 4 Hypermethylated genes associated with decreased survival rate in melanoma patients

The Kaplan-Meier curves for genes (DSP, EPHB6, HCK, IL18, IRAK3 and KIT) whose hypermethylation was associated with a lower overall survival rate (OS); the Cox proportional

univariate approach was performed on each gene to test whether a methylation status of a particular gene significantly influences the survival at the $p < 0.05$ level.

Figure 5 Relationship between gene expression and DNA methylation

The gene expressions of MCAM, FGFR3 and IL8 were measured by qRT-PCR and are presented as bars (fold change in left Y axis), and Avg-Beta methylation values are demonstrated as lines (shown in right Y axis). Methylation data was extracted from Illumina bead assay, with distinct probes represented as different lines. Gene expression differences among the groups were analysed using the Mann-Whitney test, which revealed significant differences for the MCAM and IL8 genes.

~~**Figure 6 Coincidence of DNA copy number (CN) alterations and hypermethylation**~~

~~**(A)** The distribution of CN aberrations (red indicates CN losses and green indicates CN gains on the frequency plot) specific for the $BRAF^{V600E}$ mutant (purple line on the left) and $BRAF^{V600E}$ wild-type (green line on the left) primary melanomas. The methylated genes are shown as blue lines in the lower part of the figure, and the red dotted circle highlights 6q23 as the only region where a coincidence was revealed. The significant CN alterations are highlighted in grey in the upper part of the figure. Frequent CN losses **(B)** and CN gains **(C)** are given based on the G-score, which is a measure of the frequency of occurrence of the aberration and the magnitude of the CN alteration at each location in the aggregate of all samples in the dataset. The locations of the alterations in each sample are permuted, simulating data with random aberrations, and the significance is represented as Q-Bounds. Panel **(C)** depicts the correlation plot for CN alterations and DNA methylation regarding the MYB gene and **(D)** the EYA4 gene.~~

Figure 6 Coincidence of DNA copy number (CN) alterations and disturbed methylation pattern in $BRAF^{V600E}$ mutant melanomas

(A) The distribution of CN aberrations (red indicates CN losses and blue indicates CN gains on the frequency plot) specific for the $BRAF^{V600E}$ mutant (purple line on the left) and $BRAF^{V600E}$ wild-type (green line on the left) primary melanomas. The methylated genes are shown as blue lines in the lower part of the figure, and the red dotted circle highlights 6q23 as the only region where a coincidence was revealed. The significant CN alterations are highlighted in grey in the upper part of the figure. Frequent CN losses **(B)** and CN gains **(C)** are given based on the G-score of GISTIC algorithm, which is a measure of the frequency of occurrence of the aberration and the magnitude of the CN alteration at each location in the

Formatted: Font: Not Italic

aggregate of all samples in the dataset. The locations of the alterations in each sample are permuted, simulating data with random aberrations, and the significance is represented as Q-Bounds. Grey lines indicate the peak, whereas the grey shaded area is an extended peak based on leave-one-out algorithm to allow for errors in the boundaries in a single sample. **(C)** Correlation plot for CN alterations and DNA methylation regarding the MYB gene and **(D)** the EYA4 gene.

Figure 7 FISH analysis to confirm array CGH results

CN alteration at specific regions of a representative $BRAF^{V600E}$ mutant primary melanoma: **(A)** CN gains were revealed at chromosome 6p while CN losses occurred at chromosome 6q in $BRAF^{V600E}$ samples. **(B)** High level CN gain was seen at the region of 11q13-q14. **(C)** Four colour FISH was performed to verify the CN altered genomic regions: green fluorescence (gain of CCND1 gene on 11q13), yellow fluorescence (loss of MYB gene on 6q23), red fluorescence (gain of RREB1 gene on 6p25), whereas blue fluorescence indicates centromere 6.

Supplementary Figure 1 Copy number alteration of chromosome 19 in Breslow thickness > 4 mm melanomas

(A) The Tiling Array CGH revealed characteristic CN differences among the three sample groups (pink line on the left: Breslow thickness < 2mm; yellow line: Breslow thickness 2 – 4 mm; red line: Breslow thickness > 4 mm) regarding the CN alterations of chromosome 19. The CN-altered regions involve 19p13.2 harbouring the Methyltransferase-1 gene (DNMT1). Panels **(B-E)** depict representative figures of CN losses revealed exclusively in medium- or advanced-stage (according to Breslow thickness) primary melanomas.

Table 1. Clinical-pathological parameters of primary melanomas

Variables	No. of tumoursanalysed by Illumina bead assay
All patients	42
Histological subtype	
– SSM[1]	26
– NM[2]	16
Gender	
– Female	20
– Male	22
Age (years)	
– 20-50	14
– ≥50	28
Breslow thickness (mm)[3]	
– ≤2	15
– 2-4	11
– >4	16
Location of primary tumour	
– Extremity	21
– Trunk	20
– Head	1
Metastasis formation[4]	
– Absent	20
– Present	22
Patient's survival[5]	
– Alive	21
– Exitus	21
Ulceration	
– Absent	20
– Present	22
$BRAF^{V600E}$ mutation	
– $BRAF^{V600E}$ mutant	12
– $BRAF^{V600E}$ wild type	24

[1]Superficial spreading melanoma. [2]Nodular melanoma. [3]Thickness categories are based on the current staging system. [4]Metastasis of the examined primary tumours. [5]Patients with at least a 5-year follow-up period were included.

Table 1. Clinical-pathological parameters of primary melanomas

Variables	No. of tumours analysed by Illumina bead assay
All patients	42
Histological subtype	
SSM[1]	26
NM[2]	16
Gender	
Female	20
Male	22
Age (years)	
20-50	14
≥50	28
Breslow thickness (mm)[3]	
≤4	26
>4	16
Breslow thickness (mm)[4]	
≤2	15
2-4	11
>4	16
Location of primary tumour	
Extremity	21
Trunk	20
Head	1
Metastasis formation[5]	
Absent	20
Present	22
Patient's survival[6]	
Alive	21
Exitus	21
Ulceration	
Absent	20
Present	22
$BRAF^{V600E}$ mutation	
$BRAF^{V600E}$ mutant	12
$BRAF^{V600E}$ wild type	24

[1]Superficial spreading melanoma.[2]Nodular melanoma.[3]Thickness categories are based on the current staging system. [4]Thickness categories are based on the current staging system.[5]Metastasis of the examined primary tumours. [6]Patients with at least a 5-year follow-up period were included.

RESPONSE FOR REVIEWS

First we would like to thank both Reviewers for thoroughly reviewing our manuscript. According to the suggestions of Reviewer 1, we checked our manuscript for spelling mistakes and furthermore, for the Academic Editor's requests and according to the suggestions of Reviewer 2, we reorganized some critical points in our manuscript and performed the additional signalling analysis has been requested. The title of our manuscript has been changed as well. The new title is "DNA methylation characteristics of primary melanomas with distinct biological behaviour".
It was also essential to rewrite some parts of the "Materials and Methods", "Results" and the "Discussion" sections parts. We believe that the improved version of our manuscript will meet the high standards of the PLOS One Journal.
We have answered all the comments and the questions one by one. For improved understanding we have listed the original notes and questions in bold italic and the answers in normal fonts. Among our answers, all additional descriptions we would like to add into the revised version have been marked by underlined titles and italic fonts.

REVIEWER 2

Major comments

1. The title of the manuscript is "DNA methylation is more characteristic of melanoma initiation than progression". However, the whole study did not show DNA methylation, melanoma initiation, and progression at all except for figure 2. The whole study needs to be focused on one theme.

According to the Reviewer's suggestion, the title of our manuscript was changed for "DNA methylation characteristics of primary melanomas with distinct biological behaviour".

We hope that the new title may reflect better the comprehensive analysis of our studies aiming at providing a general view in how DNA methylation associates with the distinct clinical characteristics of primary melanoma and how it accompanied by other somatic alterations. Although we attempted to evaluate whether DNA methylation contributes to other somatic alterations such as well-known mutations and copy number changes, considering possible crosstalk between the aforementioned alterations, we believe that our goals are still focused on one theme in a genomic and epigenomic scale and our results may provide improved insights into more generalized mechanisms at work in carcinogenesis.

2. Authors performed data analysis using false discovery rate cut off of 20%. Is it stringent enough?

As of yet no conventions have been established for false discovery rate (FDR) in published work, an FDR of 5 or 10% is generally chosen by studies performed at genome scale, however, considering a preselected nature of Illumina GoldenGate Cancer Panel I which is enriched in cancer related genes, a less stringent FDR value can be also acceptable [1].

3. In figure 1, authors showed the DNA methylation patterns according to different clinical predictors. What kind of data do the authors show in figure 1A? For an example, for Breslow thickness group, according to table 1, there are three size categories. Which dots are representing each class? Also where are the red dots? What

does the X axis mean? Page 9, paragraph 2, authors interpreted that "Figure 1A demonstrates that relatively large number of CpG was found to be differential methylated … in both superficial and nodular subtype." However, from the figure 1A, most of the CpG do not show significant differences at all. This figure is so confused. I can not figure out how the authors see a disturbed methylation pattern in superficial and nodular subtype (page 9).

We are very sorry if Figure 1 was not clear in the original manuscript. Figure 1A-D represent volcano plots for the methylation level of CpG sites in relation with Breslow thickness, Metastatic capacity, Ulceration and Histologic subtype. This type of plot was originally developed to illustrate gene expression data, however, several publications have chosen Volcano plots to depict differential DNA methylation data as well [2,3]. The volcano plot arranges genes along dimensions of biological and statistical significance. The first (horizontal) dimension is the relative difference between the methylation of two given groups on a log scale; consequently, hypo and hypermethylation appear symmetric. In this case, it is crucial to emphasize that samples with worse prognoses were compared to samples with better prognosis. (If samples that are characteristic for favourable prognosis are compared to samples with worse prognosis, the differentially methylated genelist will remain the same, but turn backward in position.) The second (vertical) axis represents the p-value for a t-test of differences between samples (most conveniently on a negative log scale – so smaller p-values appear higher up). For improved understanding and to avoid misleading of readers, we reedited Figure 1 in a coloured style (see below, p.3) and clearly indicated the p-value cut-off (based on t-tests corrected for FDR) by a horizontal green line, whereas vertical green line was inserted to separate direction to decreased - and increased DNA methylation (therefore, dots are not specific for samples but mark individually the differentially methylated genes). To visualize the overlap between the differentially methylated genes in each clinical subgroup, we created individual Venn diagrams specific for hypo- and hypermethylation, respectively. Notably, the new Supplementary Table 1 corroborates Figure 1 providing detailed gene lists with fold change values; the rate of fold change clearly shows if a methylation level of a given gene decrease or increase in relation with tumour progression categories.

The following text was inserted into the Results section in order to provide better description of Figure 1 (p.9, line 10):

"Figure 1A demonstrates that relatively large number of CpG sites was found to be differentially methylated between melanoma subgroups. Interestingly, the majority of these CpGs were characterised by decreased DNA methylation levels in samples with poor prognosis (larger than 4 mm, metastatic, ulcerated and nodular primary melanomas). Histologic subtype exhibited a more disturbed methylation pattern involving high number of differentially methylated genes in both superficial and nodular subtype. As it can be seen in Figure 1A, some of the differentially methylated individual genes were represented by more than one significant CpG sites arguing in favour of the consistency of given alterations. Altogether, 111 differentially methylated genes were identified in the context of aforementioned clinical predictors: 43 individual genes were hypermethylated and 68 genes hypomethylated in melanomas with less favourable clinical outcome. The differentially methylated gene lists specific for the Breslow thickness, ulceration, metastatic capacity and histologic subtype are detailed in Supplementary Table 1. Venn diagrams (Figure 1B) indicate the common properties among genes with decreased and increased DNA methylation, respectively."

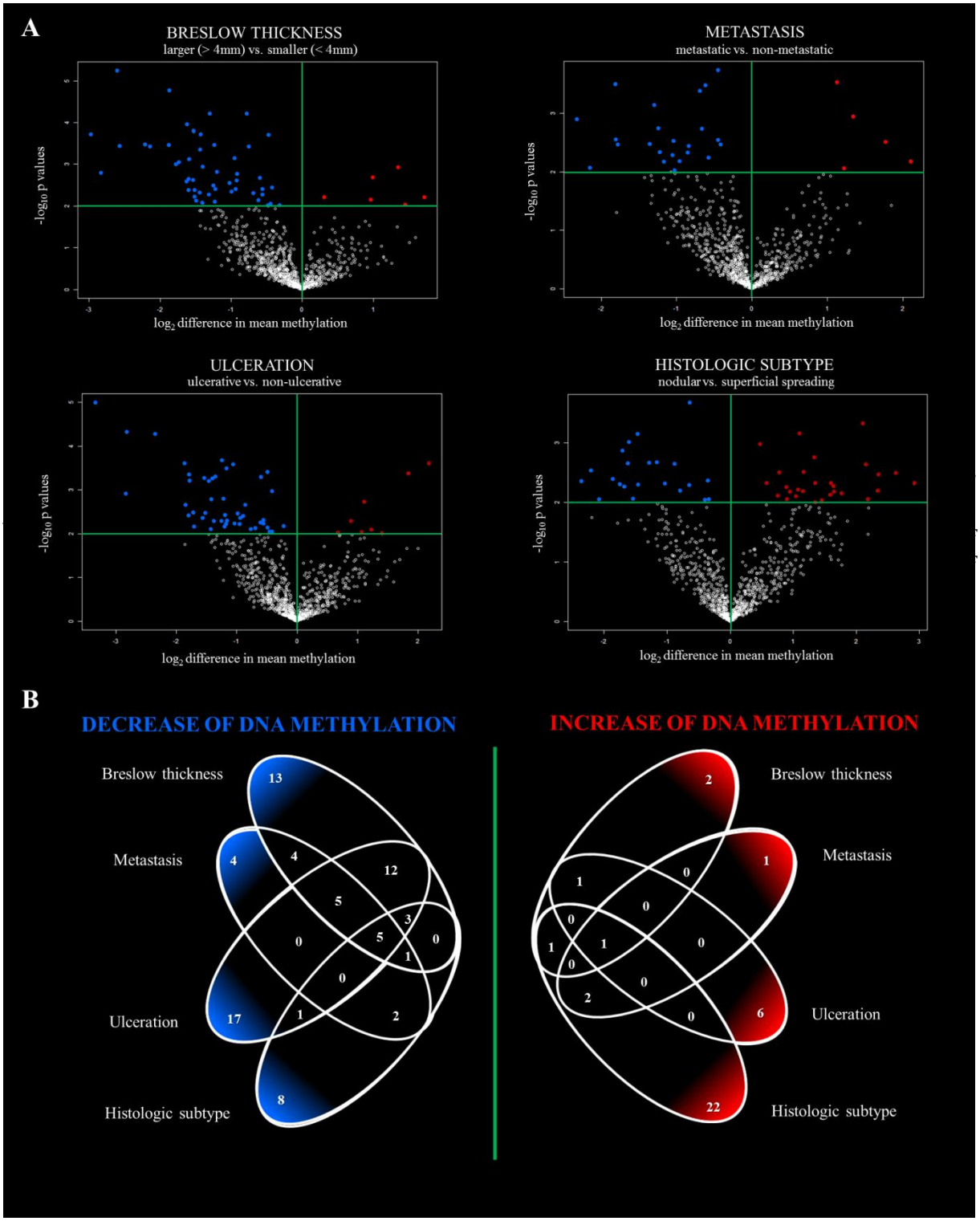

Figure 1 DNA Methylation patterns of primary melanomas with known clinical predictors
(A) *Volcano plots of differentially methylated genes associated with known predictors. Blue dots indicates decreased and red indicates increased methylation as follows: Breslow thickness: 51 hypomethylated probes (43 individual genes) and 5 hypermethylated probes (5 individual genes); metastatic capacity: 23 hypomethylated probes (21 individual genes) and 5 hypermethylated probes (4 individual genes), ulceration: 48 hypomethylated probes (43 individual genes) and 8 hypomethylated probes (8 individual genes), histologic subtype: 28 hypomethylated probes (26 individual genes) 23 hypermethylated probes (20 individual genes)* ***(B)*** *A Venn diagrams indicate the overlap of differentially methylated genes (in left: number of hypomethylated genes; in right: number of hypermethylated genes) for each clinical predictor class.*

Although the clinicopathological characteristics of primary melanomas were summarized in Table 1, regarding Breslow thickness (which is a continuous variable measured in millimetres) we further clarified it in Table 1 (see at p5) and indicated that melanoma thickness can be categorized into two or either more groups according to the clinical practise [4,5]. On binary data (each class are binary shown in Figure 1), t-test was used as indicated in the Materials and Methods section.

For better following of statistical analysis and illustrations, the following part was inserted into the "Materials and Methods" section (p.7, line 13):

Statistical analysis

"To compare the methylation patterns between primary melanoma groups detailed in Table 1, we applied random variance t-statistics on all the binary data classes such as Breslow thickness with the cut-off value of 4 mm; metastasis, ulceration and histologic subtype. Being continuous variable, Breslow thickness can be divided into more subgroups: according to the TNM system up to 5 groups can be created, however, due to the limitation of smaller samples, developing 3 groups based on the cut-off values of 2mm and 4mm were the most ideal. F-statistics was applied on the trichotomised Breslow groups for each CpG site.

CpG sites were considered differentially methylated when their p values based on univariate t-tests or f-tests were less than 0.01; in addition, given CpG sites were identified differentially methylated between the melanoma subgroups based on a multivariate permutation test providing 90% confidence that the false discovery rate was less than 20%. Volcano plots were applied to illustrate differential methylation patterns among clinical subgroups of melanomas (the clinicopathological characteristics of melanomas are summarized in Table 1). Volcano plots combine p-values of the t-tests for each CpG sites and ratios between the melanoma subgroups. Additionally, the trichotomised Breslow thickness groups were visualized by heatmap and compared by Principal Component Analysis (PCA).

For the aforementioned class comparisons, M-values, the logit transformations of signal intensities were used."

Table 1. Clinical-pathological parameters of primary melanomas

Variables	No. of tumours analysed by Illumina bead assay
All patients	42
Histological subtype	
SSM[1]	26
NM[2]	16
Gender	
Female	20
Male	22
Age (years)	
20-50	14
≥50	28
Breslow thickness (mm)[3]	
≤4	26
>4	16
Breslow thickness (mm)[4]	
≤2	15
2-4	11
>4	16
Location of primary tumour	
Extremity	21
Trunk	20
Head	1
Metastasis formation[5]	
Absent	20
Present	22
Patient's survival[6]	
Alive	21
Exitus	21
Ulceration	
Absent	20
Present	22
$BRAF^{V600E}$ mutation	
$BRAF^{V600E}$ mutant	12
$BRAF^{V600E}$ wild type	24

[1]Superficial spreading melanoma.[2]Nodular melanoma.[3]Thickness categories are based on the current staging system. [4]Thickness categories are based on the current staging system.[5]Metastasis of the examined primary tumours. [6]Patients with at least a 5-year follow-up period were included.

4. Figure 2, authors showed the differences in DNA methylation during different stages. How about DNA methylation changes for other subtypes? Also, how did authors pick the 45 CpGs? Why does the middle panel for figure 2A have fewer CpGs for the same gene?

As written above (see Answers for Question 2), the DNA methylation changes for all the subtypes of melanomas (Breslow thickness, Histological subtype, Metastatic capacity and Ulceration) were computed based on t-tests for each CpG values and adjusted for FDR and finally shown by Volcano plots which combine the p-values and fold changes between the given subgroups. Among clinical properties of melanomas, Breslow thickness is measured in millimetres. Being a continuous variable, Breslow thickness provides a unique opportunity to create more than two groups. In the clinical practice, Breslow thickness can be dichotomised by the cut-off value of 4 mm (melanomas larger than 4mm reflects the worst prognosis) or more commonly, divided into three groups by the cut-off values of 2 mm and 4 mm [4,5].

Altogether, the data in which the statistical comparison were made are the same compared to those which are indicated in Figure 1A, however, on trichotomised data, f-tests should be used instead of t-test, which results in a slightly different number of methylated genes among thin, medium and thick melanomas compared to results depicted in Figure 1A. Nonetheless, the overlap between the two approaches (statistics on dichotomised vs. trichotomised datasets) is above 80% and the latter approach provides a unique opportunity to illustrate the dynamics of DNA methylation changes over melanoma progression.

5. Authors looked at pathways without explaining how they performed the analysis. Authors should use the genes shown differences in DNA methylation in figure 2 to look for the pathways that might be perturbed during melanoma progression.

It is interest of seeing that melanoma bearing BRAF mutation has different methylated gene patterns. What is the relationship between BRAF mutation and melanoma initiation and progression? Authors should present the rationale for each analysis in the main text.

We used Efron-Tibshirani GSEA (Gene Set Enrichment Analysis) maxmean statistical approach which is implemented into BRB Array Tools Software. The entire background of GSEA maxmean test was published by Tibshirani et al [6]. Briefly, the t-statistics of z_j for all genes in our data are computed, where $\mathbf{z}k = (z1, z2, \ldots, zm)$ is the gene scores for the m genes in a geneset Sk. Then a gene-set score $Sk(\mathbf{z}k)$ for each gene-set Sk is computed equal to essentially a signed version of the Kolmogorov–Smirnov statistic between the values $\{zj, j \in Sk\}$ and their complement $\{zj, j \notin Sk\}$; the sign taken positive or negative depending on the direction of shift. The idea is that if some or all of the gene-set Sk have higher (or lower) values of zj than expected, their summary score Sk should be large. An absolute cut-off value is defined, and values of Sk above (or below) the cutoff are declared significant. The GSEA method then performs many permutations of the sample labels and recomputes the statistic on each permuted dataset.

According to the Reviewer's suggestion, besides the comparison of $BRAF^{V600E}$ and wild type melanomas, we extended our signalling analysis to each clinical subgroups and found lack of enrichment involving exclusively a single signalling pathway being enriched for ulcerated and one melanomas. Therefore, we reedited Figure 3 with legends as follows:

A

Characteristics	KEGG Pathway	Pathway description	No. of CpG probes	No. of individual genes	p-value (Efron-Tibshirani GSA test)
$BRAF^{V600E}$ mutation	hsa01430	Cell communication	21	14	< 0.005
	hsa04512	ECM-receptor interaction	17	13	0.005
Metastatic capacity	hsa04110	Cell cycle	26	24	< 0.005
Ulceration	hsa04670	Leukocyte transendothelial migration	22	17	0.005

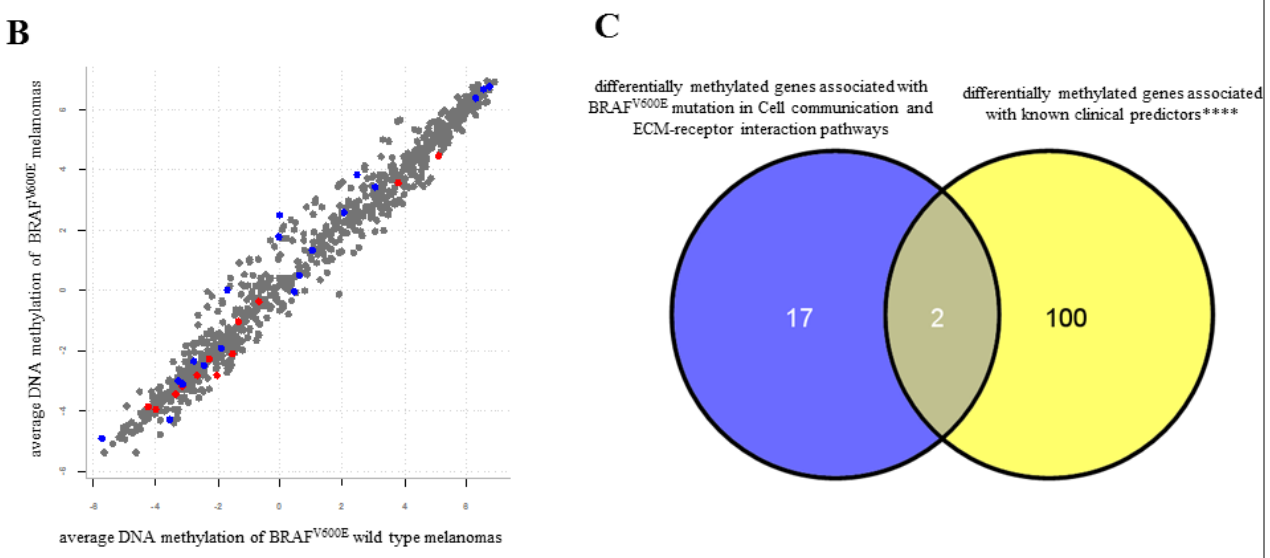

Figure 3 Differentially methylated gene sets between melanoma classes

(A) *Differentially methylated gene sets between $BRAF^{V600E}$ mutant and wild-type, metastatic and non-metastatic, ulcerated and non-ulcerated classes according to the Kyoto Encyclopaedia of Genes and Genomes.* ***(B)*** *Average log-ratios of methylation intensities in $BRAF^{V600E}$ mutant and wild-type melanomas. Red indicates significant genes associated with ECM-receptor interaction and blue depicts significant genes on Cell communication pathway. (Eleven genes overlap between the ECM-receptor interaction and Cell communication.)* ***(C)*** *Venn diagram shows lack of overlap between differentially methylated genes associated with $BRAF^{V600E}$ mutation and the known clinical predictors as Breslow thickness, metastatic capacity, ulceration and histologic subtype.*

Corrected parts of the Results section:

"In addition to individual gene signatures, we aimed to determine whether the perturbed KEGG-based gene networks are related to localised methylation patterns. We identified differentially methylated genes belongs to Cell cycle pathways in primary melanomas with metastatic capacity. Genes associated at Leukocyte signalling were also demonstrated to be differentially methylated in ulcerated samples (Figure 3A). Interestingly, Cell communication and ECM-receptor interaction networks were found to be significant at the 0.01 level between $BRAF^{V600E}$ mutant and wild type samples, notwithstanding the fact that, we was unable to find differentially methylated CpGs at the individual gene level (Figure 3A-B). The full list of CpG probes is given in Supplementary Table 2. There was poor overlap (Figure 3C) between the differentially methylated genes associated with $BRAF^{V600E}$ mutation and clinical subgroups discussed above".

Apart from the single study on melanoma cell lines – mentioned in our "Discussion" section – the association between DNA methylation and activating *BRAF* mutations in colon cancer has been identified [7]. Based on these investigations the following part has been inserted into the "Discussion" section (p.15, line 24):

"A remarkable study performed by Roon et al. revealed the $BRAF^{V600E}$ *mutation-specific hypermethylation of CpG regions in colon cancer samples by Differential Methylation Hybridization on high-density oligonucleotide microarrays. Interestingly, the authors identified several cancer-related pathways, including the PI3 kinase and Wnt signaling pathways being differentially methylated between* $BRAF^{V600E}$ *mutant and wild type samples. Additionally, the group found the silencing of* FOXD3 hypermethylated manner. *Based on these studies, authors suggest that a specific epigenetic pattern can contribute to a favorable context for the acquisition of* $BRAF^{V600E}$ *mutations. However, further studies are warranted to further clarify the relationship between the mutation and DNA methylation."*

6. Authors performed qPCR for measuring mRNA expression of a couple of genes. Authors should perform RNA-seq or microarray to measure gene expression alteration during different stages of progression.

We have to agree with the Reviewer that mRNA-seq is the most accurate method for gene expression measurement. However, we used qPCR to measure the gene expression of exclusively some of those genes that were altered by methylation. For decades, qPCR has been the gold standard for detecting mRNA expression of specific genes. Recently, RNA-seq, the robust and highly reliable method has been introduced and in the field of melanoma research the technique is still pioneering and only a few results have been published so far summarized by Dannemann et al [8]. Nonetheless, the published data on samples other than melanoma showed that RNA-seq and qPCR results highly correlated suggesting the reproducibility of qPCR experiments [9]. Apart from the numerous advantages and improved insights provided by the RNA-seq method, our goal was to validate our DNA methylation results on a gene expression level in randomly selected genes rather than provide a systematic, genome scale comparison between methylation and mRNA expression.

7. Figure legend of figure 6 needs to be clarified. Authors wrote "Red indicated CN losses and green indicated CN gains". However, where is the green? What does shaded area mean? It seems that DNA methylation is everywhere and at a similar level? Authors need to quantify the DNA methylation and CN changes. Also authors should compare that among samples from different stages in order to correlation DNA mehtyaltion, CN changes, and melanoma progression?

The copy number aberrations over all of our primary melanoma dataset were quantified according to the GISTIC (Genomic Identification of Significant Targets in Cancer), designed for analysing chromosomal aberrations specifically in cancer based on the following method:
The so-called G scores involve both the frequency of occurrence and the amplitude of the copy number aberration [10]. The algorithm also assesses the statistical significance of each aberration by comparing the observed statistic to the results that would be expected by chance, using a permutation test that is based on the overall pattern of aberrations seen across the genome. The statistical approach method adjusts for multiple-hypothesis testing using the false-discovery rate (FDR) and assigns a q value to each result, reflecting the probability that the event is due to chance fluctuation [10]. Using GISTIC, the common chromosome arm-

level events are omitted and the more informative so-called "focal events" or in other word, the "peak regions" of significance are determined (depicted by grey lines at Figure 6) with their boundaries, the so-called "extended regions" which are indicated by the grey shaded area. Calculating of the aforementioned boundaries is based on leaving each sample out in turn, and recalculating the peak boundaries.

Based on the suggestions of Reviewer 2, we corrected the legend of Figure 6 as follows:

Figure 6 Coincidence of DNA copy number (CN) alterations and disturbed methylation pattern in BRAF^{V600E} mutant melanomas

(A) *The distribution of CN aberrations (red indicates CN losses and blue indicates CN gains on the frequency plot) specific for the BRAF^{V600E} mutant (purple line on the left) and BRAF^{V600E} wild-type (green line on the left) primary melanomas. The methylated genes are shown as blue lines in the lower part of the figure, and the red dotted circle highlights 6q23 as the only region where a coincidence was revealed. The significant CN alterations are highlighted in grey in the upper part of the figure. Frequent CN losses* ***(B)*** *and CN gains* ***(C)*** *are given based on the G-score of GISTIC algorithm, which is a measure of the frequency of occurrence of the aberration and the magnitude of the CN alteration at each location in the aggregate of all samples in the dataset. The locations of the alterations in each sample are permuted, simulating data with random aberrations, and the significance is represented as Q-Bounds. Grey lines indicate the peak, whereas the grey shaded area is an extended peak based on leave-one-out algorithm to allow for errors in the boundaries in a single sample.* ***(C)*** *Correlation plot for CN alterations and DNA methylation regarding the MYB gene and* ***(D)*** *the EYA4 gene.*

With comparing copy number changes to DNA methylation results, our aim was to highlight associations between the distinct types of somatic alterations. Association was exclusively found to be related to BRAF ^{V600E} mutation. Additional copy number changes (without coordinate differentially methylation) are reported also in Figure 6 (between BRAF^{V600E} mutant and wild type samples) and in Supplementary Figure 1 (between small, medium and large primary melanomas according to the trichotomised Breslow thickness categories).

Minor comments

1. What are the M-values and Avg-Beta values? Authors should explain what they are when they first introduce in the text. The same thing for OS values for figure 4.

Based on the Reviewer's suggestion, the "Bead Assay Experiment" part of the "Materials and Methods" section has been completed as well (p.5, line 24) as the legend of Figure 4 to clearly explain the meaning of AVG-Beta values, M-values and OS.

Bead Assay experiments

"The quantitative methylation status of the 1505 CpG sites corresponding to 807 cancer-related gene promoters was determined using the Illumina GoldenGate Methylation Assay (Illumina, San Diego, CA, USA) on bisulphite-treated DNA samples corresponding to 42 primary melanomas. Bisulphite treatment was performed on 500 ng DNA using the EZ DNA Methylation-Gold Kit (Zymo Research). Duplicate samples were included to measure inter-array reproducibility for quality control. The GoldenGate assay consists of two allele-specific oligos (ASO) and two locus-specific oligos (LSO) for each CpG site. Each ASO–LSO oligo pair corresponds to either the methylated or unmethylated state of the CpG site. Each

methylation CpG spot is represented by two-color fluorescent signals from the M (methylated) and U (unmethylated) alleles. BeadStudio version 3.2 (Illumina) was used for obtaining the signal values (Avg-Beta) corresponding to the ratio of the fluorescent signal from the methylated allele (Cy5) to the sum of the fluorescents signals of both methylated (Cy5) and unmethylated alleles (Cy3), 0 corresponding to completely unmethylated sites and 1 to completely methylated sites. In agreement with the literature, 83 probes corresponding to the sex chromosomes were excluded to avoid any sex-specific bias. The probes with detection P values exceeding 0.01 in more than 10% of the specimens were removed from the analyses to exclude non-biological differences. As Du et al. performed a systematic comparison between Avg-Beta values and M-values, which is the logit transformation of Avg-Beta, and M-values were proven to be statistically valid for conducting differential methylation analysis[11], M-values were used for class comparisons, whereas the raw Avg-Beta values were applied for correlation analyses (see at "Statistical Analysis")."

Figure 4 Hypermethylated genes associated with decreased survival rate in melanoma patients

The Kaplan-Meier curves for genes (DSP, EPHB6, HCK, IL18, IRAK3 and KIT) whose hypermethylation was associated with a lower overall survival rate (OS); the Cox proportional univariate approach was performed on each gene to test whether a methylation status of a particular gene significantly influences the survival at the $p < 0.05$ level.

References

1. Hernandez-Vargas H, Ouzounova M, Le Calvez-Kelm F, Lambert MP, McKay-Chopin S, et al. (2011) Methylome analysis reveals Jak-STAT pathway deregulation in putative breast cancer stem cells. Epigenetics 6: 428-439.
2. Christensen BC, Houseman EA, Poage GM, Godleski JJ, Bueno R, et al. (2010) Integrated profiling reveals a global correlation between epigenetic and genetic alterations in mesothelioma. Cancer Res 70: 5686-5694.
3. Nischal S, Bhattacharyya S, Christopeit M, Yu Y, Zhou L, et al. (2013) Methylome profiling reveals distinct alterations in phenotypic and mutational subgroups of myeloproliferative neoplasms. Cancer Res 73: 1076-1085.
4. Fisher NM, Schaffer JV, Berwick M, Bolognia JL (2005) Breslow depth of cutaneous melanoma: impact of factors related to surveillance of the skin, including prior skin biopsies and family history of melanoma. J Am Acad Dermatol 53: 393-406.
5. Guitera P, Li LX, Crotty K, Fitzgerald P, Mellenbergh R, et al. (2008) Melanoma histological Breslow thickness predicted by 75-MHz ultrasonography. Br J Dermatol 159: 364-369.
6. Efron B TR (2007) On testing the significance of sets of genes. Ann Appl Stat: 107-129.
7. van Roon EH, Boot A, Dihal AA, Ernst RF, van Wezel T, et al. (2013) BRAF mutation-specific promoter methylation of FOX genes in colorectal cancer. Clin Epigenetics 5: 2.
8. Kunz M, Dannemann M, Kelso J (2013) High-throughput sequencing of the melanoma genome. Exp Dermatol 22: 10-17.
9. Wang Z, Gerstein M, Snyder M (2009) RNA-Seq: a revolutionary tool for transcriptomics. Nat Rev Genet 10: 57-63.
10. Beroukhim R, Getz G, Nghiemphu L, Barretina J, Hsueh T, et al. (2007) Assessing the significance of chromosomal aberrations in cancer: methodology and application to glioma. Proc Natl Acad Sci U S A 104: 20007-20012.
11. Du P, Zhang X, Huang CC, Jafari N, Kibbe WA, et al. (2010) Comparison of Beta-value and M-value methods for quantifying methylation levels by microarray analysis. BMC Bioinformatics 11: 587.